ESD-TR-72-323

MTR-2455

RADIO WAVE PROPAGATION IN THE PRESENCE OF A TROPOSPHERIC DUCT

M. R. Dresp

DECEMBER 1972

Prepared for

DEPUTY FOR PLANNING AND TECHNOLOGY

ELECTRONIC SYSTEMS DIVISION
AIR FORCE SYSTEMS COMMAND
UNITED STATES AIR FORCE
L. G. Hanscom Field, Bedford, Massachusetts

Approved for public release;
distribution unlimited.

Project 511A

Prepared by

THE MITRE CORPORATION
Bedford, Massachusetts

Contract F19628-71-C-0002

ESD-TR-72-323

MTR-2455

RADIO WAVE PROPAGATION IN THE PRESENCE OF A TROPOSPHERIC DUCT

M. R. Dresp

DECEMBER 1972

Prepared for

DEPUTY FOR PLANNING AND TECHNOLOGY

ELECTRONIC SYSTEMS DIVISION
AIR FORCE SYSTEMS COMMAND
UNITED STATES AIR FORCE
L. G. Hanscom Field, Bedford, Massachusetts

Project 511A

Prepared by

THE MITRE CORPORATION
Bedford, Massachusetts

Contract F19628-71-C-0002

FOREWORD

The work described in this report was carried out under the sponsorship of the Deputy for Planning and Technology, Project 511A, by The MITRE Corporation, Bedford, Massachusetts under Contract F19628-71-C-0002.

REVIEW AND APPROVAL

Publication of this technical report does not constitute Air Force approval of the report's findings or conclusions. It is published only for the exchange and stimulation of ideas.

NEIL P. ANDERSON, Acting Director
Communications System Plng
Deputy for Planning and Technology

ABSTRACT

A full-wave solution has been obtained for radio wave propagation in the presence of an elevated tropospheric layer. This analysis was performed as part of the CNI (Communication, Navigation, Identification) experimental program. The tropospheric layer is modeled as a trilinear refractive index profile with a sufficient lapse rate so as to result in an elevated duct. The analytical solutions give the received signal level for air-to-air propagation paths at UHF, the corresponding signal fading level, and the space diversity distance to insure good quality reception. The analysis performed here can be applied to ionospheric propagation and to the underwater acoustic channel.

ACKNOWLEDGMENT

The author is grateful to Mrs. M. T. Nowak whose expert computer programming knowledge helped make the numerical results available in such a short time.

TABLE OF CONTENTS

TABLE OF CONTENTS (Cont.)

LIST OF ILLUSTRATIONS

LIST OF TABLES

SECTION 1

INTRODUCTION

1.1 Motivation for the Problem

In the course of designing a propagation experiment for the Communication, Navigation and Identification (CNI) Program [1]*, for air-to-air and air-to-ground communications links at UHF, it was recognized that anomalous tropospheric conditions could lead to serious degradation (or enhancement) in signal strength and to multipath (interference) effects similar to those produced by the earth. These facts prompted an initial investigation into the subject of tropospheric propagation. It was learned that tropospheric layers** in the first few kilometers above ground are relatively common, but their precise effect on signal strength, fading characteristics, Doppler spectrum, available bandwidth, space diversity and relative terminal heights has been investigated in relatively few cases.

Propagation in an anomalous atmosphere has been studied extensively using the theory of geometrical optics. The theory was quite successful in explaining the gross features of the results of air-to-air propagation tests at UHF [2]. However, the theory is approximate and it suffers from the drawback of all geometrical optics treatments in that the solution breaks down at the caustics, and furthermore, cannot predict field strengths beyond the horizon. Analytical solutions or full wave solutions for elevated layer propagation have received only a few approximate and incomplete treatments. Furry [5] has obtained approximate solutions which are valid for the trapped or ducted waves only, Northover [6] has treated (at VHF) the elevated layer as a dis-

* A bibliography is listed at the end of the report.

** The term layer means a stratum, of vertical thickness from a few meters to several hundred meters, within which the mean vertical gradient and/or the variance of refractive index are much greater than elsewhere (see Section 1.2).

continuity of the index of refraction, which is an unrealistic model in the general case, and Chang [5] considered (at VHF) only the trapped waves, essentially ignoring the effects of the earth.

As a result of this initial investigation, it was seen that the present insufficient and incomplete knowledge of wave propagation at UHF in the presence of elevated layers could not lead to the effective planning of a propagation experiment. Moreover, only more precise analytical results along with a more realistic model of the layer would lead to a better interpretation of the final test data from such an experiment. It is with this objective in mind, that the present work was undertaken.

1.2 A Discussion of the Problem

We will give in this section an outline of the problem and the results we hope to obtain. We will discuss the assumptions that we are making, and delineate the part of the work that is original. We will also include a description of the troposphere and the effects of elevated layers on received signal strength.

The problem considered is that of determining the electromagnetic field produced by a vertical magnetic dipole (transmitter) in a radially inhomogeneous medium (troposphere) on or above a spherical earth. A full wave solution is obtained for the case when the variation of the index of refraction of the atmosphere is such as to produce an elevated tropospheric duct. The solutions for the field intensity are obtained as a function of frequency, layer height and vertical thickness, lapse rate or change of index of refraction with height (dN/dh) within the layer, and as function of transmitter and receiver heights and separations. In the solution of the problem the WKB or phase integral solutions for a second order ordinary differential equation are used. The work of previous authors is extended in three important ways. First, we use the "extended" WKB solutions of Langer [6]. This approach allows the closing of the "gap" in the regular WKB solutions. It involves Hankel

functions of order one-third. Second, the Langer solutions valid only for a single transition point are extended to be valid for three transition points. This is essential to obtain results valid in the elevated duct and it is accomplished by obtaining solutions in three regions and joining these at the bottom and top of the elevated layer heights. And third, the resultant solutions for the trapped and leaky waves, are obtained from the solution of a single transcendental equation. This result is, to the best of the author's knowledge, entirely original.

The refractive index profile of the troposphere is given by three linear line segments of different slope. While at first sight this choice might seem artificial, it has been shown by refractometer measurements that index of refraction profiles do take on such abrupt changes and, hence, the trilinear profile becomes a valid approximation. In reality, all that is required for the presented solutions to apply is that the profile be "sufficiently" linear in the three segments*. The second assumption we are making is to replace the spherical earth by a flat earth and modify the index of refraction, so called earth flattening approximation. In this case the solutions are valid to within two percent up to ranges of about half the radius of the earth, and this independent of the frequency. On the other hand, the error in the height-gain functions increases with elevation as $h^{5/2}$ and is proportional to the frequency [7]. At a frequency of 300 MHz and an elevation of 5000 feet, for example, the height-gain function is only in error by less than two percent. The third assumption is that the earth is a perfect conductor. This is a good approximation for horizontally polarized waves and for the low elevation angles of interest here.

We will now turn to a discussion of the troposphere and the effects of elevated ducts on communication links.

---

* The sufficiency condition is given in Section 1.3.

The elevated inversion layer or elevated duct is characterized by a rapid decrease in the index of refraction, n over a relatively short height interval. The index of refraction n can be derived from basic thermodynamic laws and can be shown to give

$$n = 1 + \left[\frac{77.6}{T} \quad (p + \frac{4810e}{T})\right] \quad 10^{-6}$$

where p is the atmospheric pressure (millibars), T is the temperature (absolute scale) and e is the partial pressure of water vapor (millibars). The refractive index of the troposphere does not to a first order approximation depend on the frequency for wavelengths longer than 1 cm. For waves of the millimeter range considerable losses appear, which can be considered by means of the introduction of a complex dielectric constant of air. Then the index of refraction n will depend on frequency. In this report we are not interested in frequencies higher than 10 GHz.

In view of the small departure of n from unity (on the order of 10^{-4}) it is often convenient to use the quantity $N = (n - 1)\ 10^{6}$, called refractivity. Near the earth's surface the index depends on the climatic and meteorological conditions and varies within 260-460 N-units. On the average, the value of N changes linearly with height, and for the middle latitudes the gradient of the change N with height h is

$$\frac{dN}{dh} \approx -40 \text{ N-units/km} .$$

An elevated layer is shown qualitatively in Figure 1.1 at an altitude between 1000 and 1100 meters.

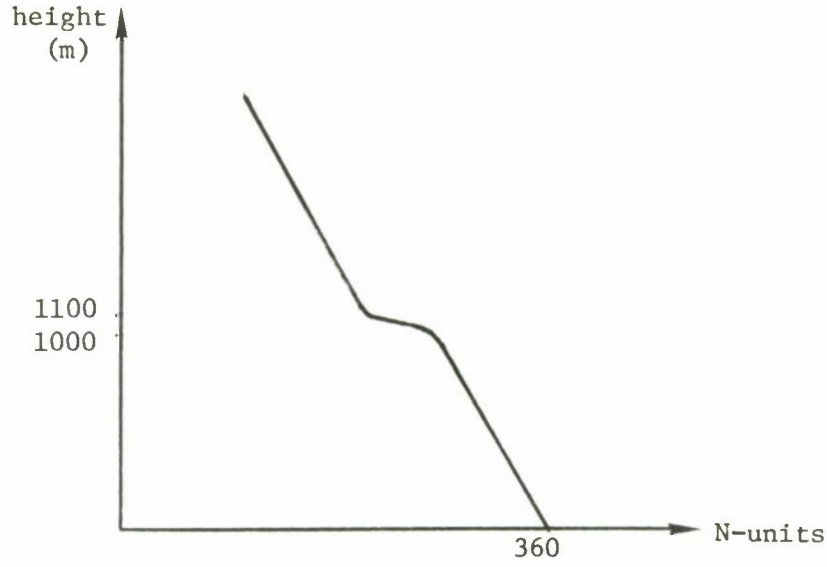

FIGURE 1.1 ELEVATED DUCT --
N-PROFILE

Most frequently these layers are caused by a mass of warm dry air overlying a cool moist air mass. The usual occurrence of this phenomenon is at heights of approximately 1 to 2 kilometers. When the refractivity gradient exceeds 157 N-units/km, within the layer, the layer becomes an elevated duct. The changes in N have been measured to be as high as 5×10^3 N-units per km. Sometimes 20-25 N-unit changes have been measured across a layer having a thickness of a few meters only.

Even though, the modified index or earth flattening procedure has certain limitations as pointed out above, it offers great simplification and a large insight into duct propagation. For this reason, we will use the concept of the modified index of refraction to give a qualitative description of propagation in elevated ducts. The modified index of refraction seeks to accomplish two aims: (1) its vertical gradient should vanish at any elevation for which the path of a ray launched horizontally is a circular arc concentric with the surface of the earth;

and (2) it should be readily calculable from the refractivity N. For this reason the modified index is defined by [8],

$$M(h) = N + 10^6 \frac{h}{a}$$

where h is the height above the earth and a is the radius of the earth.

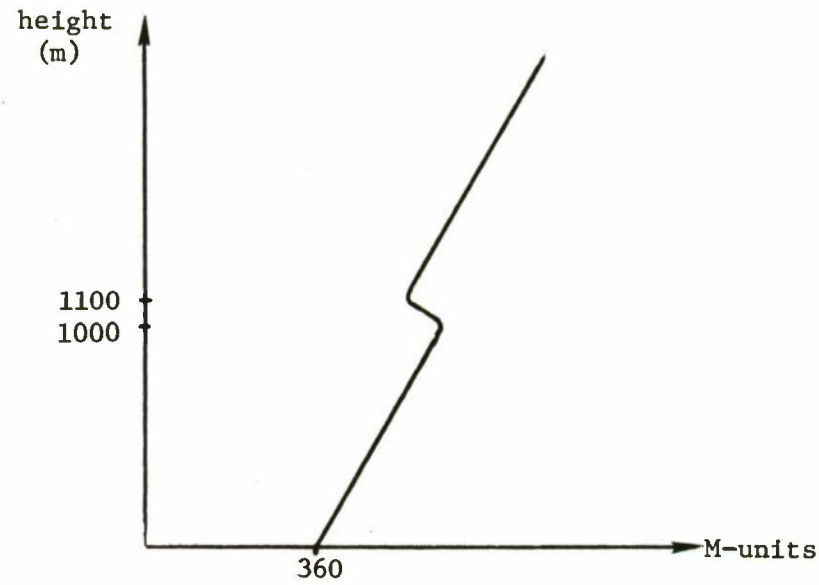

FIGURE 1.2 ELEVATED DUCT --
M - PROFILE

In a distribution in which M is constant rays are straight, when dM/dh is negative rays curve downward and when dM/dh is positive, the rays are refracted upward. The net result is that through the use of M(h) a spherical coordinate problem is more simply analyzed in rectangular coordinates, where plane wave modes have replaced spherical-harmonic modes. An M-profile roughly corresponding to the N-profile of Figure 1.1 is illustrated. We will use a profile similar to Figure 1.2 in the solution of our problem.

The disturbing effect of tropospheric ducts on air-to-air and air-to-ground communication links has been investigated in several important experiments [9, 10, 11]. In general three types of disturbances have been observed which cannot be explained in terms of ground reflections and which are evidently associated with the tropospheric propagation medium. These disturbances are (i) intervals of range in which average signal has decreased 15 or 20 dB (radio-holes), (ii) intervals of range in which the average signal exceeds the free-space value by 10 or 12 dB (anti-holes) and (iii) intervals in range in which interference type of lobes (multipath) of large amplitude (10-20 dB) appear. It has been observed that radio holes and anti-holes occurring far from within to far beyond the standard horizon are very common air-to-air. For instance, all of the 50 air-to-air propagation flights made by Wright Air Development Center in 1951-1953 encountered radio holes; these flights were made under fair weather during May-October in a three year period in Ohio [9]. Radio holes far within the standard horizon are not so common ground-to-air.

1.3 Outline of Approach

The procedure is to reduce the problem of determining the electric field strength of a dipole anywhere in space to the solution of an inhomogeneous Hertzian potential wave equation with radial and angular coordinate dependence. The solution is subject to the boundary condition at the earth, the Sommerfeld radiation condition, the continuity of the solution plus its derivative at all non-singular points and the condition that the solution must remain finite at the dipole source. By separation of variables the Hertzian potential is represented as an infinite sum of radial and angular dependent functions. The angular functions are Legendre functions and the radial functions are as yet unspecified. The coefficients of the summation can be obtained from the boundary conditions. The resulting series is, however, a very slowly converging series. To improve the rate of convergence of this series the Watson transformation is applied. The individual terms of this resulting series are evaluated at the roots for which the Wronskian vanishes. This will give a general solution.

The refractive index profile is then chosen as to give three transition points; this corresponds to an elevated duct. The radial dependent functions mentioned above are evaluated by an approximate solution to the radial wave equation with the "extended WKB" method due to Langer [6], at each transition point and in three separate regions. The solutions are Bessel functions. The solutions in the three regions are then joined by the continuity conditions. The fact is then emphasized that the propagation problem reduces to the solution of an eigenvalue problem for an ordinary differential equation. Hence, the solution has to satisfy the boundary condition at the surface of the earth and the radiation condition at infinity. The resulting set of complex eigenvalues and the associated eigen-functions represent a complete set of solutions to the problem. Substituting this set of eigenvalues and eigen-functions in the general series solution, we can determine the field strength due to the radiating dipole at any point in space.

In the solution of this problem it will be seen that an eigenvalue ordinary differential of the form occurs:

$$\frac{d^2u_n}{dh^2} + k_o^2 [y(h) + \lambda_n] u_n = 0 \qquad (1.1)$$

where λ_n and u_n are the eigenvalues and eigenfunctions, respectively, $k = 2\pi/\lambda$, and $y(h)$ is related to the modified index of refraction by $y(h) = 2 \times 10^{-6} (M(h) - M_o)$. The functions u_n must satisfy the boundary condition at the earth and the radiation condition at infinity. The form of the solution to this differential equation will depend upon the term in brackets and in particular upon the eigenvalues λ_n which are in general complex. When the λ_n have imaginary parts (positive) which are comparable in magnitude to their real parts, the corresponding wave is said to be "leaky". This is because the value of the function $u_n(h)$ is found to increase rapidly with height. When the imaginary part of λ_n becomes small and the real part of λ_n is comparable to $(-M(h_c))$ (see Figure 1.1), we have "transitional" waves. And when the imaginary part of $\lambda_n \approx -M(h_b)$, the waves are "trapped", because the functions $u_n(h)$ has its largest value between h_a and h_c. We will use the "extended" WKB (Wentzel, Kramers, Brillouin) solutions of equation (1.1) in the three cases of leaky, transitional, and trapped waves.

In general, the term $[y(h) + \lambda_n]$ vanishes at three points which, though complex, are extremely close to the real values h_1, h_2, h_3 shown in Figure 1.1.

Such points are called turning points or transition points. This description has its origin in quantum mechanics where an equation very similar to equ. (1.1), namely Schrödinger's equation, has been the subject of considerable analysis. The solutions of this equation make a transition from, say oscillatory to exponential at the transition point.

The Jeffreys, Wentzel, Kramers, Brillouin (JWKB) or WKB method is a procedure for finding approximate solutions to a second order differ-

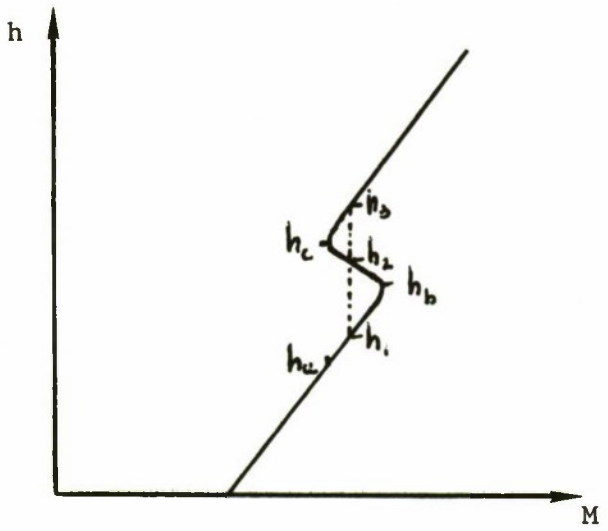

FIGURE 1.3 M-PROFILE

ential equation of the form

$$u'' + f(z)u = 0 \tag{1.2}$$

in some region, R, in which f(z) is analytic and contains no zeros, and in which f(z) varies sufficiently slowly. This means that the first two derivatives of f have to be sufficiently small throughout the region in question, with $f \neq 0$ therein [4]. The WKB solution of (1.2) is given by

$$u = f^{-\frac{1}{4}} \left(Ae^{iF(z)} + Be^{-iF(z)}\right) \tag{1.3}$$

where

$$F(z) = \int_{z_o}^{z} f^{\frac{1}{2}}(\zeta)\, d\zeta \tag{1.4}$$

and A and B are arbitrary constants.* However, the WKB approximation always fails sufficiently near a zero of f(z). A form of the solution of (1.2) which is valid up to the zero of f(z) itself was given by R. E. Langer [6]. This solution has the form

$$u = \left(\frac{F}{F'}\right)^{\frac{1}{2}} \left\{ A\, H^{(1)}_{1/3}(F) + B\, H^{(2)}_{1/3}(F) \right\} \tag{1.5}$$

where F = F(z) is as defined above and A and B are arbitrary constants, and the $H_{1/3}$ are Hankel functions of the first and second kind. This approximation satisfies the equation

$$u'' + \left(Q^2 - \frac{5}{36}\frac{Q^2}{F^2} + \frac{3}{4}\frac{Q'^2}{Q^2} - \frac{1}{2}\frac{Q''}{Q} \right) u = 0 \tag{1.6}$$

where $Q = f^{\frac{1}{2}}$. Hence, if we can show that

$$\frac{3}{4}\frac{Q'^2}{Q^2} - \frac{5}{36}\frac{Q^2}{F^2} - \frac{1}{2}\frac{Q''}{Q} << Q^2 \tag{1.7}$$

the solution in (1.5) is a very good approximation of the original differential equation (1.2).

A limitation of the Langer WKB solution extension is that the method applies only to a single transition point. Hence, in our approach to the problem we shall obtain "extended" WKB solutions of the differential equation in a region including only one transition point. These solutions are then "joined" at the border of each region by employing the continuity of the functions and their derivatives, so that the general solution is valid in the semi-infinite interval extending from the surface of the earth to infinity.

---

* Northover [5], p. 37ff, shows that for the WKB solution to hold we must have $|f'/f^{3/2}| << 1$ and $f''/f^{1/2} << 1$.

1.4 Contents of the Report

We will give here a brief outline of the remainder of this report. In Section 2, we formulate the problem in a precise mathematical way. The three dimensional vector solutions of Maxwell's equations are reduced to a one dimensional vector by the introduction of the Hertz potential. By placing the transmitting source on the polar axis, advantage is taken of the symmetry of the problem. As a result, the Hertz potential has only an r and θ dependence. The electric and magnetic fields can then be written in terms of this Hertz potential. In Section 3, we obtain the slowly converging series solutions for the Hertz potential. By separation of variables this series can be written as the product of the radial dependent, r and angular dependent, θ functions. The angular functions are Legendre polynomials, and the radial functions are as yet unspecified; since they depend on the particular index of refraction profile assumed. In Section 4, we apply the Watson transformation to obtain a more rapidly converging solution. This is done by expressing the series solution for the potential as a contour integral in the complex plane enclosing an infinite number of singularities. By Cauchy's residue theorem, the more rapidly converging series for the potential is now a sum over the residues enclosed by the contour. In Section 5, we use Langer's "extended" WKB solutions to obtain approximate solutions of the radial dependent functions. And in Section 6, we obtain the radial dependent solutions for three transition points. In Section 7, we transform these radially dependent solutions from that of a spherical geometry into a "flat earth" geometry. In Section 8, we present a model for the layered troposphere. And in Section 9, we obtain the expression for the Hertz potential and the electric field. In Section 10 we give the numerical results for the potential. The discussion in this section includes details of the numerical evaluations. Section 11 contains a summary. Relegated to the Appendices are the mathematical details of the contour integral representation and the modified Hankel functions. Also included there is the justification

for representing the three dimensional vector solutions of Maxwell's equations by the one dimensional Hertz potential.

SECTION 2

PRECISE MATHEMATICAL FORMULATION OF THE PROBLEM*

We assume the earth to be a sphere of radius a, and introduce spherical polar coordinates r, θ, φ as defined in Figure 2.1. We are given a vertical magnetic dipole of moment $m\ell$ with a harmonic time variation $e^{i\omega t}$ at a point D(b, 0, 0) and we are required to determine the electromagnetic field at an arbitrary point P(r, θ, φ) on or above the surface of the earth and at a distance $R = (r^2 + b^2 - 2br \cos \theta)^{1/2}$ from D. We assume the earth to be immersed in an inhomogeneous medium whose dielectric constant k is a function of radial distance r only, $k = k(r)$; all effects of the ionosphere have been neglected**. Inside the earth k(r) is assumed to be a constant, k_2. In any medium the propagation constant is $i\kappa = [i\omega\mu\ (\sigma + i\omega\varepsilon)]^{1/2}$ so that in air $k_o = 2\pi/\lambda$, while in the earth $k_2 = k_o\ (K - 60\ i\sigma\lambda)^{1/2}$, where K is the relative dielectic constant, σ is the conductivity (in mhos per meter) and the permeability μ is assumed to be the same inside and outside the earth. In this problem $k^2(r) = \omega^2\ \mu\varepsilon(r)$ for the troposphere.

The electromagnetic field must satisfy Maxwell's equations, both inside and outside the earth, it must possess at the point D a singularity corresponding to that of the dipole, the electric field and magnetic field must be continuous everywhere, while at infinity the field vectors must satisfy the Sommerfeld radiation condition.

Let $\overline{E}$ and $\overline{H}$ represent the electric and magnetic field vectors, respectively; the factor exp ($i\omega t$) being understood throughout. Then Maxwell's equations in m.k.s units, become the following:

---

* The material in this and the following sections is part of the author's dissertation for the Ph.D. at the University of Pennsylvania, Philadelphia.

** It has been shown experimentally that at frequencies higher than 30 MHz the ionosphere has negligible effects on terrestrial wave propagation.

IA-37,818

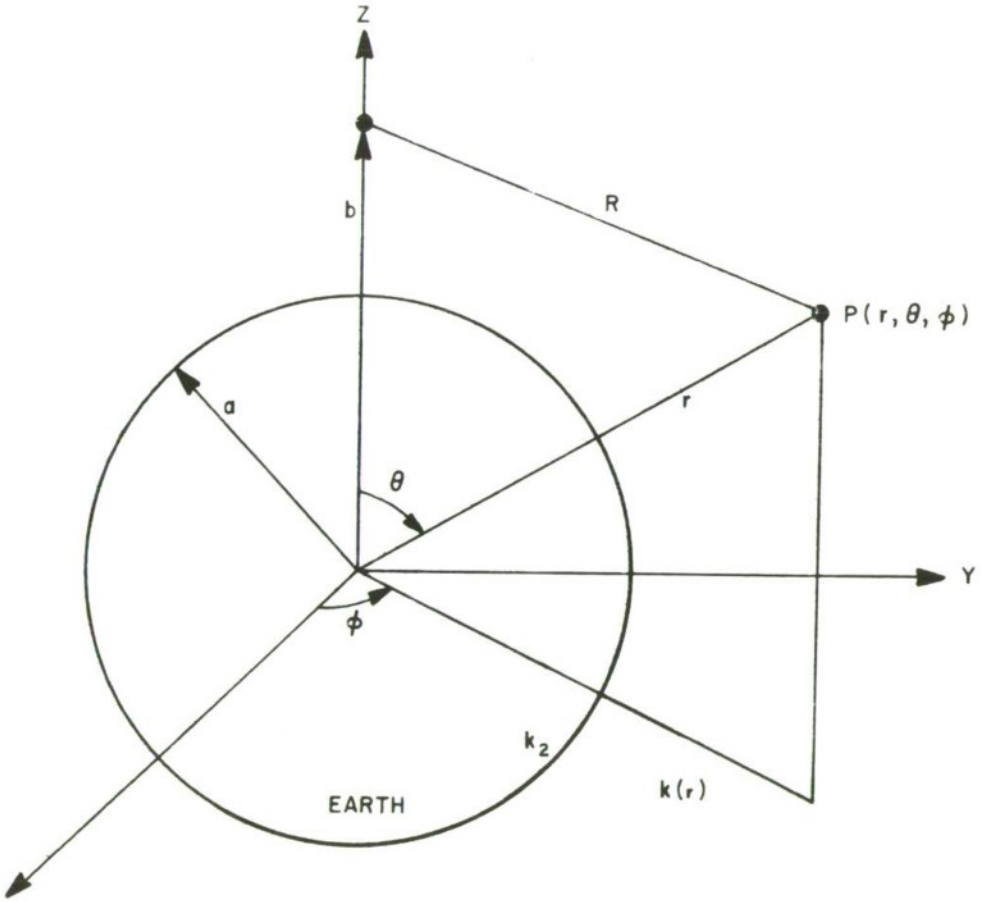

Figure 2.1 PROBLEM GEOMETRY

$$\nabla \times \overline{E} = -i\omega\mu\overline{H} \qquad \nabla \cdot \overline{H} = 0$$
$$\nabla \times \overline{H} = i\omega\varepsilon\overline{E} \qquad \nabla \cdot \varepsilon\overline{E} = 0. \tag{2.1}$$

It has been shown by Friedman [12] that in spherical coordinates the electromagnetic field given by (2.1) can be obtained from a Hertz vector $\overline{\Pi}$ which has only its radial component non-zero, even when the dielectric constant is a function of r. Since the dipole is located on the polar axis, symmetry exists, and the vector $\overline{\Pi}$ will not depend on φ but only on the coordinates r,θ. We define $\overline{\Pi} = (rU(r,\theta),0,0)$. In terms of U the electric and magnetic fields are:

$$E_r=0,\ E_\theta=0,\ H_\phi=0 \qquad E_\phi = -i\omega\mu \frac{\partial U}{\partial \theta}$$
$$H_\theta = -\frac{1}{r}\frac{\partial^2(rU)}{\partial r \partial \theta} \qquad H_r = -(k^2 + \frac{\partial^2}{\partial r^2})\ (rU). \tag{2.2}$$

Equations (2.2) represent the field of a magnetic dipole and are satisfied for

$$U = M \frac{e^{-ikR}}{4\pi R} \tag{2.3}$$

where M is proportional to the magnetic moment of the dipole, its value being

$$M = \frac{IS}{b} \tag{2.4}$$

where I is the electric current in the loop of area S and b is the distance from the center of the earth to the dipole.

The scalar wave function $U(r,\theta)$ must satisfy several conditions. First $U(r,\theta)$ must satisfy the partial differential equation

$$\text{I.} \qquad \nabla^2 U + k^2 U = 0 \tag{2.5}$$

in the exterior region $r > a$, except at the dipole, and in the interior region $r < a$. Second,

$$\text{II.} \qquad U \text{ and } \frac{\partial}{\partial r}(rU) \tag{2.6}$$

must be continuous everywhere except at the source. Thirdly, as $R \to 0$

$$\text{III.} \qquad U \to M \frac{e^{-ik(b)R}}{4\pi R} \quad . \tag{2.7}$$

This means that in the neighborhood of the dipole the potential U becomes that of an oscillating dipole in an homogeneous medium whose permittivity is equal to the local value at the dipole position. Finally, U must satisfy the Sommerfeld radiation condition given by

$$\text{IV.} \qquad \lim_{r\to\infty} r \left(\frac{\partial U}{\partial r} + ik_o U\right) = 0 \quad . \tag{2.8}$$

The fact that $U(r,\theta)$ possesses a singularity at the dipole, $r = b$, $\theta = 0$, while otherwise it satisfies the wave equation (2.5), can be expressed very concisely using the Dirac δ-function. We write

$$\nabla^2 U + k^2 U = -M \frac{\delta(r-b)\delta(\theta)}{2\pi r^2 \sin\theta} \tag{2.9}$$

where M is the source strength and the factor $2\pi r^2 \sin\theta$ is designed to normalize the solution.

SECTION 3

SERIES SOLUTION OF THE SPHERICAL HERTZIAN WAVE EQUATION

We shall now obtain a general solution to the inhomogeneous Hertzian potential wave equation given by (2.9), subject to the required boundary conditions discussed in the previous section. Rather than writing the total field as the sum of a primary field due to the dipole source and a scattered field due to the earth, we shall use a self-consistent method. In particular, we will show that the solution to the inhomogeneous wave equation (2.9) has the form of an expansion in zonal harmonics,

$$U(r,\theta) = \sum_{n=0}^{\infty} \left(\frac{2n+1}{2}\right) u_n(r)\, P_n(\cos\theta) \tag{3.1}$$

where n are integer values and $u_n(r)$ are solutions to the equation

$$\frac{d^2(ru_n)}{dr^2} + \left[k^2(r) - \frac{n(n+1)}{r^2}\right] (ru_n) = \frac{-M}{2\pi r}\,\delta\,(r-b), \tag{3.2}$$

or

$$\frac{d^2u_n}{dr^2} + \frac{2}{r}\,\frac{du_n}{dr} + \left[k^2(r) - \frac{n(n+1)}{r^2}\right] u_n = \frac{-M}{2\pi r}\,\delta\,(r-b)\,. \tag{3.3}$$

To show this we use the orthogonality property of the Legendre polynomials $P_n(\cos\theta)$ in (3.1) and find that

$$u_n(r) = \int_0^{\pi} U(r,\theta)\, P_n(\cos\theta) \sin\theta\, d\theta\,. \tag{3.4}$$

If we multiply equation (2.9) (for spherical coordinate system) by $P_n(\cos\theta)\sin\theta\, d\theta$ and integrate between 0 and π, this equation transforms into the ordinary differential equation (3.2).

The foregoing implies that for $U(r,\theta)$ given by (3.1) to be a solution of the inhomogeneous wave equation (2.9), the coefficients $u_n(r)$ must satisfy eq. (3.2). Furthermore, since the Legendre polynomials form a complete set, $U(r,\theta)$ as given by (3.1) is uniquely specified. Hence, $U(r,\theta)$ given by eq. (3.1) is the total solution of the inhomogeneous wave equation.

The boundary conditions that had been imposed on U in Section 2 must now be satisfied by (ru_n), namely

1. (ru_n) and $\frac{d}{dr}(ru_n)$ must be continuous
2. u_n must be regular at $r = 0$
3. The Sommerfeld radiation condition

$$\lim_{r\to\infty} \left|\frac{d}{dr}(ru_n) - ik_o(ru_n)\right| = 0$$

must be satisfied.

In order to solve equation (3.2) we must know the solutions of the homogeneous differential equation

$$\frac{d^2}{dr^2}(ru_n) + \left[k^2(r) - \frac{n(n+1)}{r^2}\right](ru_n) = 0 \quad . \tag{3.5}$$

When $k^2(r) = k_o^2$, a constant (case of airless atmosphere), the solutions of (3.5) are linear combinations of the Hankel functions of half-integer order, namely $H^{(1)}_{n+1/2}(r)$ and $H^{(2)}_{n+1/2}(r)$. If $k^2(r)$ is not a constant, the solutions of (3.5) behave like Bessel functions, but their exact behavior will depend on the variation of $k(r)$ with r.

3.1 General Solution for the Radial Functions

We let

$$u_n(r) = a_n V_n(r) \qquad \text{for } r \leq b$$
$$u_n(r) = b_n Q_n(r) \qquad \text{for } r \geq b$$

where the $V_n(r)$ and $Q_n(r)$ are independent solutions of the homogeneous differential equation in (3.5). They, furthermore, satisfy the required boundary condition in their respective domains. The general solution (3.1) is then given by

$$U(r,\theta) = \sum_{n=0}^{\infty} \left(\frac{2n+1}{2}\right) P_n (\cos\theta) \begin{cases} a_n V_n(r) & r < b \\ b_n Q_n(r) & r > b \,. \end{cases} \tag{3.6}$$

The coefficients a_n and b_n may be determined by applying the required boundary condition at $r = b$. At $r = b$, the functions (ru_n) are continuous and their derivatives have a junp of magnitude $-M/2\pi\, b$. From the definition of $V_n(r)$ and $Q_n(r)$ above, the functions $u_n(r)$ are regular at $r = 0$ and satisfies the radiation condition. Then we can prove that

$$a_n = \frac{-M}{2\pi W_n} Q_n(b) \tag{3.7}$$

$$b_n = \frac{-M}{2\pi W_n} V_n(b) \tag{3.8}$$

where W_n is the Wronskian of (rQ_n) and (rV_n) evaluated at $r = b$. Substituting (3.7) and (3.8) in (3.6), we obtain

$$U(r,\theta) = \frac{-M}{4\pi} \sum_{n=0}^{\infty} \frac{(2n+1)}{W_n} P_n (\cos\theta) \begin{cases} Q_n(b)\, V_n(r) & r \leq b \\ Q_n(r)\, V_n(b) & r \geq b \,. \end{cases} \tag{3.9}$$

This is the solution to our problem in its most general form for an arbitrary variation of the index of refraction of the atmosphere. Equation (3.9) represents Greens' function for the inhomogeneous wave equation (2.9). The general requirement of the reciprocity of Greens' function is satisfied owing to the fact that eq. (3.9) is symmetric in

r and b. The reciprocity with respect to angles θ and θ_o (we considered the case in which the latter is zero) can be expressed by replacing cos θ by cos $(\theta - \theta_o)$ which is symmetric in θ and θ_o. It has been shown that the solution (3.9) can be used for numerical computation only if ka is small compared to unity. For example, at 100 MHz about a million terms are required to evaluate the series. In the following sections the solution (3.9) will be transformed so that it can be readily computed for large values of ka.

SECTION 4

THE WATSON TRANSFORMATION

The series expression for $U(r,\theta)$ is very slowly converging. For example, for ka of the order of 10^6, where $k = 2\pi/\lambda$ and a is the radius of the earth, approximately 10^6 terms of the series are required to evaluate the value of $U(r,\theta)$ at one point. Such numerical calculations are even prohibitive in this age of high speed computers. A way around this laborious task was found by Watson [13]. Watson showed that the series (3.9) can be expressed as a contour integral in the complex plane enclosing an infinite number of singularities. By Cauchy's residue theorem this integral is then equal to the sum of the residues enclosed by the contour. The net effect of the Watson transformation is to have a much faster converging series. The difficulty that is left, is to locate the singularities, namely zeros of the Wronskian (see Appendix B). From eq. (B.12) we have the series representation

$$U(r,\theta) = \frac{M}{2} \sum_{\nu} \frac{\nu + \frac{1}{2}}{\sin \nu\pi} \frac{P_\nu(\cos(\pi - \theta))}{\left(\frac{dW_s}{ds}\right)_{s=\nu}} \begin{cases} Q_\nu(b)\, V_\nu(r) & r \leq b \\ Q_\nu(r)\, V_\nu(b) & r \geq b \end{cases} \tag{4.1}$$

where ν represents the zeros of the Wronskian W_s and the derivative (d/ds) is with respect to the complex variable s.

The residue

$$\frac{\nu + \frac{1}{2}}{\sin \nu\pi} \frac{P_\nu(\cos(\pi - \theta))}{W_\nu'} Q_\nu(b)\, V_\nu(r) \tag{4.2}$$

where

$$W_\nu' = \frac{d}{ds} W_s \Big|_{s=\nu} \tag{4.3}$$

can be interpreted in another way. Since the Wronskian $W_s = 0$, the two functions $Q_\nu(r)$ and $V_\nu(r)$ are linearly dependent, that is $V_\nu(r) = \alpha\, Q_\nu(r)$. This means that the function $Q_\nu(r)$, besides satisfying the Sommerfeld radiation condition, also satisfies the condition of regularity at $r = 0$. It follows that ν is an eigenvalue and $Q_\nu(r)$ is an eigenfunction of the following problem:

Find the values of ν for which $V(r)$, the solution of the differential equation:

$$\frac{d^2(rV)}{dr^2} + \left[k^2(r) - \frac{\nu\,(\nu + 1)}{r^2}\right](rV) = 0 \tag{4.4}$$

is regular at $r = 0$ and satisfies the radiation condition at infinity, that is

$$\lim_{r\to\infty} \left|\frac{d}{dr}\,(rV) - ik_o(rV)\right| = 0\ . \tag{4.5}$$

It will be seen in later sections that the zeros of the Wronskian, ν, will be very large, of the order of magnitude of ka. This allows us to use asymptotic formulas for the Legendre functions $P_\nu(\cos\,(\pi - \theta))$. We have

$$P_\nu(\cos\,\theta) \sim \left(\frac{2}{\pi(\nu+1)\,\sin\,\theta}\right)^{1/2} \cos\,\left[(\nu + \tfrac{1}{2})\,\theta - \tfrac{\pi}{4}\right] \tag{4.6}$$

for large ν, so that

$$\frac{P_\nu(-\cos\,\theta)}{\sin\,\nu\pi} = \frac{P_\nu(\cos\,(\pi - \theta))}{\sin\,\pi\nu}$$

$$\sim -\left(\frac{2i}{\pi(\nu + 1)\,\sin\,\theta}\right)^{1/2} \exp\,\{-i\,(\nu + \tfrac{1}{2})\,\theta\}\ . \tag{4.7}$$

Next, using the fact that the dielectric constant of the earth is constant, it has been shown [12] that the boundary condition at the surface of the earth can be written as

$$\left[\frac{\partial}{\partial r}\,(rV_s) - \Gamma\,(rV_s)\right]_{r=a} = 0 \tag{4.8}$$

$$\Gamma = i(k_2^{\,2} - k_o^{\,2})^{1/2}$$

where k_2 and k_o are the wave-numbers of the earth and free space, respectively. A perfectly conducting earth implies $k_2 = \infty$ and hence (4.8) reduces to

$$(rV_s)\Big|_{r=a} = 0\ . \tag{4.10}$$

Equation (4.8) can also be written in a preferred form:

$$\left(\frac{\frac{\partial}{\partial r}\,(rV_s)}{(rV_s)}\right)\Bigg|_{r=a} = \Gamma\ . \tag{4.11}$$

We shall use this result presently.

It is shown in Appendix C, that with the aid of equations (4.10) and (4.11), the expression (4.1) can be written for an inhomogeneous earth and a perfectly conducting earth, respectively, as

$$U(r,\theta) = \frac{M}{4a^2}\sum_{\nu}\frac{(2\nu+1)}{\sin\,\nu\pi}\,\frac{Q_\nu(b)\,Q_\nu(r)}{Q_\nu(a)\,Q_\nu(a)}\,\frac{P_\nu(\cos\,(\pi-\theta))}{\left[\frac{\partial}{\partial t}\,\frac{\frac{d}{dr}\,(rQ_t)}{rQ_t}\right]_{\substack{r=a\\ t=\nu}}} \tag{4.12}$$

$$U(r,\theta) = \frac{-M}{4br} \sum_{\nu} \frac{(2\nu+1)}{\sin \nu\pi} \frac{(bQ_\nu(b))(rQ_\nu(r))}{\left[\frac{d}{dr}(rQ_\nu)\right]} \frac{P_\nu(\cos(\pi - \theta))}{\left[\frac{\partial}{\partial t}(rQ_t)\right]_{\substack{r=a \\ t=\nu}}} \cdot \tag{4.13}$$

Using the approximation (4.7), we obtain

$$U(r,\theta) = \frac{-M}{a^2} \sum_{\nu} \left[\frac{(2\nu+1)\, i}{\pi \sin \theta}\right]^{1/2} \exp\left[i\left(\nu + \tfrac{1}{2}\right)\theta\right] \cdot \tag{4.14}$$

$$\frac{Q_\nu(b)\, Q_\nu(r)}{Q_\nu(a)\, Q_\nu(a)} \cdot \frac{1}{\left[\frac{\partial}{\partial t} \frac{\frac{d}{dr}(rQ_t)}{rQ_t}\right]_{\substack{r=a \\ t=\nu}}}$$

and

$$U(r,\theta) = -M \sum_{\nu} \frac{(2\nu+1)\, i}{\pi \sin \theta}^{1/2} \exp\left[i\left(\nu + \tfrac{1}{2}\right)\theta\right] \cdot$$

$$\frac{Q_\nu(b)\, Q_\nu(r)}{\left[\frac{d}{dr}(rQ_\nu)\right]_{r=a} \left[\frac{\partial}{\partial t}(rQ_t)\right]_{\substack{r=a \\ t=\nu}}} \cdot \tag{4.15}$$

Equation (4.14) and (4.15) are the expressions for the Hertz potential satisfying the boundary condition (4.11) and (4.10), respectively.

The formulation in (4.14) (also (4.15)) has the advantage that the same formula for $U(r,\theta)$ represents $r > b$ and $r < b$, in contrast

to eq. (4.1). The expression, however, breaks down for $\theta = 0$ since for small θ,

$$P_\nu(-\cos\theta) \to \frac{\sin \nu\pi}{\pi} \log \theta^2$$

whereas the function P_ν represents is to be regular for $\theta = 0$ and $r \neq b$. It implies that the whole "ray" $\theta = 0$ must be considered a singularity of the representation in (4.14) and (4.15). This condition, however, presents no problem in this investigation, since we will always be interested in fields well removed from the $\theta = 0$ line.

SECTION 5

THE LANGER APPROXIMATE FORMULAS

In Section 4 it was shown that the problem of determining the Hertz vector $U(r,\theta)$ and then the electromagnetic field depends upon the solution of the eigenvalue problem for the differential equation (4.4). In this section we will discuss the "extended" WKB approximations due to Langer to obtain solutions of this differential equation. The extended form is valid in the neighborhood of the transition point as well as at the transition point itself.

Langer has demonstrated that the solutions of the so called related second order ordinary differential equation for a single transition point, i.e., a zero of $[\phi^2(z) - \omega(z)]$ in eq. (5.1),

$$g(z) + [\phi^2(z) - \omega(z)]\, g(z) = 0 \tag{5.1}$$

is given by

$$g(z) = \Psi(z)\, \zeta^{1/3}\, H_{1/3}^{(j)}(\zeta) \qquad j = 1, 2 \tag{5.2}$$

in which the symbols $H_{1/3}^{(j)}$ stand for the Hankel functions of order 1/3, of the j^{th} kind, and

$$\Psi(z) = \zeta^{1/6}(z)\, \phi^{-1/2}(z) \tag{5.3}$$

$$\zeta(z) = \int_{z_1}^{z} \phi(z)\, dz \tag{5.4}$$

$$\omega(z) = \frac{\Psi''(z)}{\Psi(z)} \tag{5.5}$$

where z_1 is a zero of $[\phi^2(z) - \omega(z)]$.

Although the formula for $\Psi(z)$ seems to assign a singularity to this function at z_1, it is found that this singularity is removable, and the $\Psi(z_1)$ is then different from zero. The function $\omega(z)$ is thus bounded in a region about z_1.

If it can be shown that $\omega(z)$ is very small compared to $\phi^2(z)$ over the considered region of z, then (5.2) may be considered as a solution of eq. (5.1) to practical accuracy. In that case

$$g(r) = rQ_\nu(r) \ , \tag{5.6}$$

and

$$\phi^2(r) = k_o^2 \left[k^2(r) - \frac{\nu(\nu+1)}{k_o^2 r^2}\right] . \tag{5.7}$$

In the region of the zero, if

$$|\phi^2(r)| << 1 \ , \tag{5.8}$$

then the condition

$$|\omega(z)| << 1 \tag{5.9}$$

must be satisfied for (5.6) to be an approximate solution to the wave equation. If these conditions are satisfied in the interval of interest, for which there is only a single transition point at $r = r_1$, then the general solution is given by

$$rQ_\nu = \left(\frac{\zeta(r)}{\phi(r)}\right)^{1/2} \left[A_\nu H_{1/3}^{(1)}(\zeta) + B_\nu H_{1/3}^{(2)}(\zeta)\right] \tag{5.10}$$

where

$$\zeta = \int_{r_1}^{r} \phi \, dr \tag{5.11}$$

and $\phi(r)$ is given by (5.7). Thus eq. (5.10) represents the approximate solution in the region that includes one transition point. For the regions of the second and third transition point, solutions of a similar form apply, each valid only in a region including one transition point.

It has been shown that if ϕ^2 is linearly varying, $\omega(z_1) = 0$ and hence eq. (5.9) is satisfied as well as the condition $|\omega(z)| << \phi^2(z)$ for all z.

Furthermore, Langer has shown that for large ζ the asymptotic forms of the Hankel functions may be used. Hence

$$H_{1/3}^{(1)}(\zeta) = C_1 \frac{e^{i\zeta}}{\zeta^{1/2}} \tag{5.12}$$

$$H_{1/3}^{(2)}(\zeta) = C_2 \frac{e^{-i\zeta}}{\zeta^{1/2}} \tag{5.13}$$

where C_1 and C_2 are constants that depend on the normalization of these functions. If (5.12) and (5.13) are substituted in (5.10), we obtain

$$rQ_\nu = C_3 \frac{e^{i\int_{r_1}^{r} \phi \, dr}}{\phi^{1/2}} + C_4 \frac{e^{-i\int_{r_1}^{r} \phi \, dr}}{\phi^{1/2}} \quad . \tag{5.14}$$

It may be recognized that (5.14) are the "ordinary WKB" solutions. This form of the solution, however, breaks down at a zero of ϕ^2.

For the discussion of conditions on the permittivity when ϕ^2 is not varying linearly the reader is referred to Doviak and Goldhirsh [14] and Bremmer [15].

SECTION 6

SOLUTIONS FOR THREE TRANSITION POINTS

As we have mentioned in the previous section the extended WKB solutions are valid in a region including only one transition point. It was pointed out in the Introduction that for the problem of the elevated duct, three transition points exist. Hence we must obtain three separate solutions for each of the three regions. These solutions are then matched at points between the transition points using the continuity boundary conditions.

We will represent the solutions (rQ_ν) to the homogeneous wave equation in regions I, II and III by $(rQ_\nu)_1$, $(rQ_\nu)_2$ and $(rQ_\nu)_3$, respectively. Region I extends from r = a to $r = \eta_1$, region II for $\eta_1 \leq r \leq \eta_2$, and region III from $r = \eta_2$ to infinity. Since $(rQ_\nu)_3$ must satisfy the Sommerfeld radiation condition, only solutions $H^{(2)}_{1/3}$ are allowed. Hence, we have in Region I:

$$(rQ_\nu)_1 = A_\nu \left(\frac{\zeta_1}{\phi_1}\right)^{1/2} H^{(1)}_{1/3}(\zeta_1) + B_\nu \left(\frac{\zeta_1}{\phi_1}\right)^{1/2} H^{(2)}_{1/3}(\zeta_1); \quad (6.1)$$

in region II:

$$(rQ_\nu)_2 = C_\nu \left(\frac{\zeta_2}{\phi_2}\right)^{1/2} H^{(1)}_{1/3}(\zeta_2) + D_\nu \left(\frac{\zeta_2}{\phi_2}\right)^{1/2} H^{(2)}_{1/3}(\zeta_2); \quad (6.2)$$

in region III:

$$(rQ_\nu)_3 = F_\nu \left(\frac{\zeta_3}{\phi_3}\right)^{1/2} H^{(2)}_{1/3}(\zeta_3) ; \quad (6.3)$$

where

$$\zeta_1(r) = \int_{r_1}^{r} \phi(r)\, dr$$

$$\zeta_2(r) = \int_{r_2}^{r} \phi(r)\, dr \tag{6.5}$$

$$\zeta_3(r) = \int_{r_3}^{r} \phi(r)\, dr \tag{6.6}$$

$(rQ_\nu)_j$ and $(rQ_\nu)_j'$ (j = 1,2,3) (prime means differentiation with respect to r) must be continuous at $r = \eta_1$ and $r = \eta_2$. The coefficients A_ν, B_ν, C_ν and D_ν may be expressed only in terms of F_ν. Further, let

$$\lambda^{(1)}_{1\eta 1} = \left(\frac{\zeta_{1\eta 1}}{\phi_1}\right)^{1/2} H^{(1)}_{1/3}(\zeta_{1\eta 1}) \tag{6.7}$$

$$\lambda^{(2)}_{1\eta 1} = \left(\frac{\zeta_{1\eta 1}}{\phi_1}\right)^{1/2} H^{(2)}_{1/3}(\zeta_{1\eta 1}) \tag{6.8}$$

$$\lambda^{(1)}_{2\eta 1} = \left(\frac{\zeta_{2\eta 1}}{\phi_{21}}\right)^{1/2} H^{(1)}_{1/3}(\zeta_{2\eta 1}) \tag{6.9}$$

$$\lambda^{(2)}_{2\eta 1} = \left(\frac{\zeta_{2\eta 1}}{\phi_{21}}\right)^{1/2} H^{(2)}_{1/3}(\zeta_{2\eta 1}) \tag{6.10}$$

$$\lambda^{(1)}_{2\eta 2} = \left(\frac{\zeta_{2\eta 2}}{\phi_{22}}\right)^{1/2} H^{(1)}_{1/3}(\zeta_{2\eta 2}) \tag{6.11}$$

$$\lambda^{(2)}_{2\eta 2} = \left(\frac{\zeta_{2\eta 2}}{\phi_{22}}\right)^{1/2} H^{(2)}_{1/3}(\zeta_{2\eta 2}) \tag{6.12}$$

$$\lambda^{(2)}_{3\eta 2} = \left(\frac{\zeta_{3\eta 2}}{\phi_{32}}\right)^{1/2} H^{(2)}_{1/3}(\zeta_{3\eta 2}) \tag{6.13}$$

where

$$\zeta_{1\eta 1} \equiv \int_{r_1}^{\eta_1} \phi dr \tag{6.14}$$

$$\zeta_{2\eta 1} \equiv \int_{r_2}^{\eta_1} \phi dr \tag{6.15}$$

$$\zeta_{2\eta 2} \equiv \int_{r_2}^{\eta_2} \phi dr \tag{6.16}$$

$$\zeta_{3\eta 2} \equiv \int_{r_3}^{\eta_2} \phi dr \ . \tag{6.17}$$

Using the above in equations (6.1) to (6.3) and applying continuity conditions at η_1 and η_2 we have the set of four simultaneous equations

$$A_\nu \lambda_{1\eta 1}^{(1)} + B_\nu \lambda_{1\eta 1}^{(2)} = C_\nu \lambda_{2\eta 1}^{(1)} + D_\nu \lambda_{2\eta 1}^{(2)} \tag{6.18}$$

$$A_\nu \lambda_{1\eta 1}^{(1),} + B_\nu \lambda_{1\eta 1}^{(2),} = C_\nu \lambda_{2\eta 1}^{(1),} + D_\nu \lambda_{2\eta 1}^{(2),} \tag{6.19}$$

$$C_\nu \lambda_{2\eta 2}^{(1)} + D_\nu \lambda_{2\eta 2}^{(2)} = F_\nu \lambda_{3\eta 2}^{(2)} \tag{6.20}$$

$$C_\nu \lambda_{2\eta 2}^{(1),} + D_\nu \lambda_{2\eta 2}^{(2),} = F_\nu \lambda_{3\eta 2}^{(2),} \tag{6.21}$$

which gives for A_ν and B_ν

$$A_\nu = K_{\nu_1} F_\nu \tag{6.22}$$

$$B_\nu = K_{\nu_2} F_\nu \tag{6.23}$$

where

$$+K_{\nu_1} = -\left[\frac{\lambda^{(2)}_{1\eta 1}\,\lambda^{(2)}_{3\eta 2}\,L_1 + \lambda^{(2)}_{1\eta 1}\,\lambda^{(2)}_{3\eta 2}\,L_2 + \lambda^{(2)}_{1\eta 1}\,\lambda^{(2)}_{3\eta 2}\,L_3 + \lambda^{(2)}_{1\eta 1}\,\lambda^{(2)}_{3\eta 2}\,L_4}{D}\right] \tag{6.24}$$

where

$$D \equiv \left[\lambda^{(1)}_{1\eta 1}\,\lambda^{(2)}_{1\eta 1} - \lambda^{(1)}_{1\eta 1}\,\lambda^{(2)}_{1\eta 1} \quad \lambda^{(1)}_{2\eta 2}\,\lambda^{(2)}_{2\eta 2} - \lambda^{(1)}_{2\eta 2}\,\lambda^{(2)}_{2\eta 2}\right] \tag{6.25}$$

and

$$K_{\nu_2} = \frac{\lambda^{(1)}_{1\eta 1}\,\lambda^{(2)}_{3\eta 2}\,L_1 + \lambda_{1\eta 1}\,\lambda_{3\eta 2}\,L_2 + \lambda^{(1)}_{1\eta 1}\,\lambda^{(2)}_{3\eta 2}\,L_3 + \lambda^{(1)}_{1\eta 1}\,\lambda^{(2)}_{3\eta 2}\,L_4}{D} \tag{6.26}$$

where

$$L_1 = \lambda^{(1)}_{2\eta 1}\,\lambda^{(2)}_{2\eta 2} - \lambda^{(2)}_{2\eta 1}\,\lambda^{(1)}_{2\eta 2}, \tag{6.27}$$

$$L_2 = \lambda^{(1)}_{2\eta 1}\,\lambda^{(2)}_{2\eta 2} - \lambda^{(1)}_{2\eta 1}\,\lambda^{(1)}_{2\eta 2} \tag{6.28}$$

$$L_3 = \lambda^{(2)}_{2\eta 1}\,\lambda^{(1)}_{2\eta 2} - \lambda^{(1)}_{2\eta 1}\,\lambda^{(2)}_{2\eta 2}, \tag{6.29}$$

$$L_4 = \lambda^{(2)}_{2\eta 1}\,\lambda^{(1)}_{2\eta 2} - \lambda^{(1)}_{2\eta 1}\,\lambda^{(2)}_{2\eta 2}\ . \tag{6.30}$$

The functions L_1, L_2, L_3 and L_4 depend only on the layer between η_1 and η_2. It will be seen later that this interval $\eta_1 < \eta < \eta_2$ also corresponds to the tropospheric layer.

Substituting (6.24) and (6.26) into (6.1) gives

$$(rQ_\nu) = F_\nu \left[K_{\nu_1} \left(\frac{\zeta_1}{\phi_1}\right)^{1/2} H^{(1)}_{1/3}(\zeta_1) + K_{\nu_2} \left(\frac{\zeta_1}{\phi_1}\right)^{1/2} H^{(2)}_{1/3}(\zeta_1) \right] . \tag{6.31}$$

Substituting this in the boundary condition at the earth, we obtain

$$\left. \frac{\frac{\partial}{\partial r}\left[\left(\frac{\zeta_1}{\phi_1}\right)^{1/2} H^{(2)}_{1/3}(\zeta_1) - k \left(\frac{\zeta_1}{\phi_1}\right)^{1/2} H^{(1)}_{1/3}(\zeta_1) \right]}{\left[\left(\frac{\zeta_1}{\phi_1}\right)^{1/2} H^{(2)}_{1/3}(\zeta_1) - k \left(\frac{\zeta_1}{\phi_1}\right)^{1/2} H^{(1)}_{1/3}(\zeta_1) \right]} \right|_{r=a} = \Gamma \tag{6.32}$$

where

$$k = -K_{\nu_1} / K_{\nu_2} . \tag{6.33}$$

In the case of a perfectly conducting earth $\Gamma = \infty$, and equation (9-32) reduces to

$$\left[\left(\frac{\zeta_1}{\phi_1}\right)^{1/2} H^{(2)}_{1/3}(\zeta_1) - k \left(\frac{\zeta_1}{\phi_1}\right)^{1/2} H^{(1)}_{1/3}(\zeta_1) \right]_{r=a} = 0 \tag{6.34}$$

or

$$\left. \frac{H^{(2)}_{1/3}(\zeta_1)}{H^{(1)}_{1/3}(\zeta_1)} \right|_{r=a} = k . \tag{6.35}$$

If (6.22) and (6.23) are substituted into (4.14) the coefficient F_ν in no way enter the expression $U(r,\theta)$.

SECTION 7

MODIFICATION OF THE RADIAL DIFFERENTIAL EQUATION

The next step is to obtain solutions of the homogenous differential equation (3.5). We will write equ. (3.5) in the following form:

$$\frac{d^2u_n}{dr^2} + \frac{2}{r}\frac{du_n}{dr} + \left[k^2(r) - \frac{n(n+1)}{r^2}\right] u_n = 0 \quad . \tag{7.1}$$

Letting h = r-a and substituting in (7.1), we have

$$\frac{d^2u_n}{dh^2} + \left[k_o^2\, k^2\,(h) - \frac{a^2k^2_n}{(h+a)^2}\right] u_n = 0 \tag{7.2}$$

where we have written $a^2k^2_n$ for $n(n+1)$.

Now

$$\frac{a^2k^2_n}{(h+a)^2} \approx k^2_n \left(1 - \frac{2h}{a}\right) \quad , \tag{7.3}$$

so that equation (7.2) becomes

$$\frac{d^2u_n}{dh^2} + \left[k_o^2\, k^2(h) - k_n^2 + 2k_n^2\,\frac{h}{a}\right] u_n = 0 \quad . \tag{7.4}$$

Since usually,

$$k(h) \approx 1 \tag{7.5}$$

and

$$k_n \cong k_o \tag{7.6}$$

the part in brackets in equation (7.4) becomes

$$k_o^2 k^2(h) + 2k_n^2 \frac{h}{a} = k^2 N^2(r) \tag{7.7}$$

to within terms of the order of h^2/a^2, and

$$N(r) = \frac{rk(r)}{ak_a} \quad . \tag{7.8}$$

Letting

$$N^2(h) \equiv 1 + y(h) \tag{7.9}$$

$$y(h) = 2 \times 10^{-6} [M(h) - M_o] \tag{7.10}$$

and

$$k_n^2 = k_o^2 (1 - \lambda_n) \quad , \tag{7.11}$$

we obtain for equation (7.1)

$$\frac{d^2 u_n}{dh^2} + k_o^2 [y(h) + \lambda_n] u_n = 0 \quad . \tag{7.12}$$

The effect of this transformation has been to transform the spherical earth problem into the so called "flat earth" problem. The resulting differential equation (7.12) turns out to be more easily solvable. In the case when the index of refraction varies linearly with height, the solutions of equation (7.12) take on particularly simple forms. The price one pays is that the solutions will have an error of approximately 2% for the frequencies and elevations of interest here. This we will tolerate.

In terms of the function Q_ν in the general solution (5.10), equ. (7.12) becomes

$$\frac{d^2 Q_\nu(h)}{dh^2} + k_o^2 \, [y(h) + \lambda_\nu] \, Q_\nu(h) = 0 \quad . \tag{7.13}$$

The general solution of equ. (7.13) is

$$Q_\nu(h) = \left(\frac{\zeta(h)}{\phi(h)}\right)^{1/2} [A_\nu \, H_{1/3}^{(1)} \, (\zeta(h)) + B_\nu \, H_{1/3}^{(2)} \, (\zeta(h))] \tag{7.14}$$

where

$$\zeta(h) = \int_{h_1}^{h} \phi(h) \, dh \tag{7.15}$$

and

$$\phi(h) = k_o \, [y(h) + \lambda_\nu] \quad . \tag{7.16}$$

Next, we will write the Hankel functions of order one-third, $H_{1/3}(\zeta)$ in terms of the Furry modified Hankel functions h(z). Some of the properties of these functions are given in Appendix E. Thus, the transformation is

$$h_i(z) = \zeta^{1/3}(h)\, H^{(i)}_{1/3}(\zeta(h)) \tag{7.17}$$

where

$$z = \left(\frac{3}{2}\zeta(h)\right)^{2/3} \tag{7.18}$$

$$\zeta(h) = \frac{2}{3} z^{3/2}, \tag{7.19}$$

and equ. (7.14) becomes

$$Q_\nu(h) = \frac{\zeta^{1/6}(h)}{\phi^{1/2}(h)} \left[A_\nu h_1(z) + B_\nu h_2(z)\right] . \tag{7.20}$$

This form of the solution to equation (7.1) will be used in all subsequent calculations. The remaining equations of Section 5 and Section 6 are transformed in a straight forward if somewhat tedious way. In particular equation (6.35) now takes the form

$$\left.\frac{h_2(z(h))}{h_1(z(h))}\right|_{h=0} = k . \tag{7.21}$$

SECTION 8

MODEL FOR THE TROPOSPHERE

As we have seen previously, a smoothly varying index of refraction with an elevated layer will, in general, result in the occurrence of three transition points. Instead of an analytic function for the index of refraction, we will choose three linear line segments which intersect at the heights h_1 and h_2, as in Figure 8.1. The heights h_1 and h_2 correspond to those of η_1 and η_2 in Section 6. These are the height at which we "joined" the solutions in the three regions.

h_1 is the height of the layer and $(h_2 - h_1)$ is its thickness. Mathematically, the model can be described as,

$$y(h) = \begin{cases} y_0 + a_1 h & 0 \leq h \leq h_1 \\ y_1 + a_2(h - h_1) & h_1 \leq h \leq h_2 \\ y_2 + a_1(h - h_2) & h \geq h_2 \end{cases} . \tag{8.1}$$

We have chosen the same slope (standard) for y(h) in region I and III. The slope a_2 in region II is simply given by

$$a_2 = \frac{y(h_2) - y(h_1)}{h_2 - h_1} . \tag{8.2}$$

The model y(h) is illustrated in Figure 8.2.

For this choice of model the variables ζ in equ. (6.4) to (6.6) and (6.14) to (6.17) take on the form

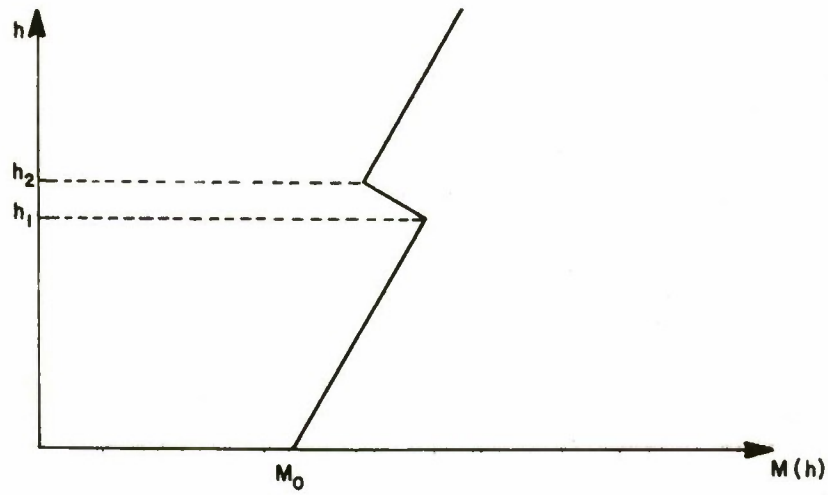

Figure 8.1 LAYER MODEL

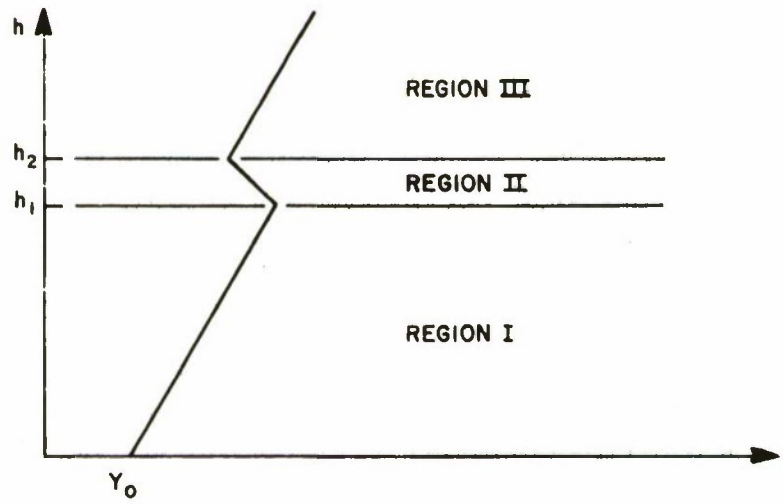

IA-37,819

Figure 8.2 THE FUNCTION Y(h).

$$\zeta_1(h) = k_o \int_{h_{01}}^{h} [y_o + a_1 h + \lambda_n]^{1/2} \, dh \tag{8.3}$$

$$\zeta_2(h) = k_o \int_{h_{02}}^{h} [y_1 + a_2 (h - h_1) + \lambda_n]^{1/2} \, dh \tag{8.4}$$

$$\zeta_3(h) = k_o \int_{h_{03}}^{h} [y_2 + a_1 (h - h_2) + \lambda_n]^{1/2} \, dh, \tag{8.5}$$

and

$$\zeta_{11}(h_1) = \frac{2}{3} \left(\frac{k_o}{a_1}\right) [y_1 + \lambda_n]^{3/2} \tag{8.6}$$

$$\zeta_{21}(h_1) = \frac{2}{3} \left(\frac{k_o}{a_2}\right) [y_1 + \lambda_n]^{3/2} \tag{8.7}$$

$$\zeta_{22}(h_2) = \frac{2}{3} \left(\frac{k_o}{a_2}\right) [y_2 + \lambda_n]^{3/2} \tag{8.8}$$

$$\zeta_{32}(h_2) = \frac{2}{3} \left(\frac{k_o}{a_1}\right) [y_2 + \lambda_n]^{3/2}. \tag{8.9}$$

In terms of the variable z defined in equ. (7.18), we have for equ. (8.6) to (8.9)

$$z_{11} = \left(\frac{k_o}{a_1}\right)^{2/3} (y_1 + \lambda_n) \tag{8.10}$$

$$z_{21} = \left(\frac{k_o}{a_2}\right)^{2/3} (y_1 + \lambda_n) \tag{8.11}$$

$$z_{22} = \left(\frac{k_o}{a_2}\right)^{2/3} (y_2 + \lambda_n) \tag{8.12}$$

$$z_{32} = \left(\frac{k_o}{a_1}\right)^{2/3} (y_2 + \lambda_n) \, . \tag{8.13}$$

Since, for the model of Figure 8.2, a_2 is negative, we will choose the principal root, that is

$$z_{21} = e^{-i\frac{2\pi}{3}} \left|\frac{k_o}{a_2}\right|^{2/3} (y_1 + \lambda_n) \tag{8.14}$$

and

$$z_{22} = e^{-i\frac{2\pi}{3}} \left|\frac{k_o}{a_2}\right|^{2/3} (y_2 + \lambda_n) \, . \tag{8.15}$$

In terms of this model, the solution $Q_\nu(h)$, equ. (7.20), takes the following form in region I:

$$Q_\nu(h) = \left(\frac{2}{3a_1 k_o^{\,2}}\right)^{1/6} \left\{ A_\nu h_1 \left(\left(\frac{k_o}{a_1}\right)^{2/3} (y_o + a_1 h + \lambda_\nu) \right) \right. \tag{8.16}$$

$$\left. + B_\nu h_2 \left(\left(\frac{k_o}{a_1}\right)^{2/3} (y_o + a_1 h + \lambda_\nu) \right) \right\}$$

for $0 \leq h \leq h_1$;

in region II:

$$Q_\nu(h) = \left(\frac{2}{3a_2k_o^2}\right) \left\{ C_\nu h_1 \left(\left(\frac{k_o}{a_2}\right)^{2/3} (y_1 + a_2(h - h_1) + \lambda_\nu) \right) + \right. \tag{8.17}$$

$$\left. D_\nu h_2 \left(\left(\frac{k_o}{a_2}\right) (y_1 + a_2(h - h_1) + \lambda_\nu) \right) \right\}$$

for $h_1 \leq h \leq h_2$;

and in region III :

$$Q_\nu(h) = \left(\frac{2}{3a_1k_o^2}\right)^{1/6} F_\nu h_2 \left(\left(\frac{k_o}{a_1}\right)^{2/3} (y_2 + a_1(h - h_2) + \lambda_\nu) \right) \tag{8.18}$$

for $h \geq h_2$.

Expressions (8.16) to (8.18) are substituted in the transcendental equation (7.21) and solved for the eigenvalues λ_ν.

SECTION 9

EXPRESSION FOR THE ELECTRIC FIELD

In terms of the function and variables defined in Section 7 and 8, the expression for the potential $U(r,\theta)$ in equation (4.13) takes the form

$$U(h,\theta) = \frac{-M}{4a^2} \sum_{\nu} \frac{2\nu + 1}{\sin \nu\theta} \frac{Q_\nu(h_o)\, Q_\nu(h)\, P_\nu(\cos(\pi - \theta))}{\left[\frac{d}{dh} Q_\nu(h)\right]_{h=0} \left[\frac{\partial}{\partial t} Q_\nu(h)\right]_{\substack{h=0 \\ t=\nu}}} \tag{9.1}$$

where ν is related to λ_ν by

$$\nu = k_o a\left(1 - \frac{1}{2}\lambda_\nu\right) \tag{9.2}$$

and

$$\frac{\partial}{\partial t} = \frac{-2}{k_o a} \frac{\partial}{\partial \lambda_\nu} \tag{9.3}$$

and h_o refers to the height of the transmitter.

The coefficients A_ν and B_ν can be related to k using equ. (6.22) and (6.23) and (6.32). Thus the expression for the height function $Q_\nu(h)$, equ. (8.16) becomes in region I

$$Q_\nu(h) = F_\nu K_{\nu_2} \left(\frac{2}{3a_1 k_o^2}\right)^{1/6} \left[h_2\left(\left(\frac{k_o}{a_1}\right)^{2/3} (y_o + a_1 h + \lambda_\nu)\right) - k\, h_1\left(\left(\frac{k_o}{a_1}\right)^{2/3} (y_o + a_1 h + \lambda_\nu)\right)\right] \tag{9.4}$$

for $0 \leq h \leq h_1$.

Similarly, the coefficients C_ν and D_ν can be written in terms of $F_\nu K_{\nu_2}$. However, in the present investigation we will limit ourselves to determining the fields above and below the layer. For $h \geq h_2$, we have

$$Q_\nu(h) = F_\nu \left(\frac{2}{3a_1 k_o^2}\right)^{1/6} h_2 \left(\left(\frac{k_o}{a_1}\right)^{2/3} (y_2 + a_1(h - h_2) + \lambda_\nu)\right) \tag{9.5}$$

for $h \geq h_2$.

Substituting equation (9.4) into (9.1) and carrying out the necessary differentiations, we obtain the following expression for the potential below the layer,

$$U = \frac{-M}{4\alpha^2 a^{4/3} (k_o\rho)^{1/3}} \sum_\nu \frac{\nu + \frac{1}{2}}{\sin \nu\pi} P_\nu (\cos(\pi - \theta)) \cdot$$

$$\left\{(h_1(0)h_2(h_0) - h_2(0)h_1(h_0))(h_1(0)h_2(h) - h_2(0)h_1(h))/\right.$$

$$\left.\left[1 - \frac{i}{\alpha(k_o a\rho)^{2/3}} k' h_1^2(0)\right]\right\} \tag{9.6}$$

for $0 \leq h \leq h_1$.

The notation $h_i(0)$, $h_2(h_0)$ and $h_i(h)$ refers to the value of the Hankel function at the values of $h = 0$, $h = h_0$ and $h = h$, respectively, in equ. (9.4). In this derivation use was made of the Wronskian

$$h_1(\zeta_1)\, h_2'(\zeta_1) - h_1'(\zeta_1)\, h_2(\zeta_1) = -\alpha i \tag{9.7}$$

where $\alpha = 1.457495$. The coefficient ρ is related to a_1 by

$$a_1 = \frac{1}{\rho a} \tag{9.8}$$

ρ is equal to (2/3) for the standard (4/3) earth atmosphere. In equ. (9.6) k' is the derivative of k with respect to the eigenvalue λ_ν.

Since ν is of the order of $k_o a$, we can make use of the asymptotic expressions for the Legendre functions of large order.

In that case,

$$\frac{(\nu + \frac{1}{2})\, P_\nu(\cos(\pi - \theta))}{\sin \nu\pi} \cong \left(\frac{2k_o a}{\pi \sin\theta}\right)^{1/2} \exp\left[i\frac{3\pi}{4} - i(\nu + \tfrac{1}{2})\,\theta\right]. \tag{9.9}$$

In future discussions it will be of interest to compare the potential U to its free space value. The value of U is

$$U_o = \frac{M}{4\pi}\,\frac{e^{-ik(b)R}}{R}. \tag{9.10}$$

If we approximate the distance R by $a\theta$ and make use of equ. (9.9) in equ. (9.6), we obtain

$$\frac{U}{U_o} = \left(\frac{\theta}{\sin\theta}\right)^{1/2} e^{+i\frac{3\pi}{4}} e^{-i\frac{1}{2}\theta\left[2\pi\,(k_o a)^{1/3}\theta\right]^{1/2}} \cdot \sum_{\nu} e^{i\frac{1}{2}k_o a\,\theta\,\lambda_\nu} \cdot$$

$$\frac{(h_1(0)h_2(h_0) - h_2(0)h_1(h_0))(h_1(0)h_2(h) - h_2(0)h_1(h))}{\left[1 - \frac{i}{\alpha(k_o a\rho)^{2/3}}\, k'\, h_1^{\,2}\,(0)\right]} \qquad (9.11)$$

for $0 \leq h \leq h_1$. The eigenvalues λ_ν are obtained from

$$\frac{h_2\left(\left(\frac{k_o}{a_1}\right)^{2/3}\lambda_\nu\right)}{h_1\left(\left(\frac{k_o}{a}\right)^{2/3}\lambda_\nu\right)} = k \qquad (9.12)$$

where k is given by equation (6.32).

The electric field E_ϕ is obtained from U by using the expression

$$E_\phi = -i\omega\mu\,\frac{\partial U}{\partial\theta} \qquad (9.13)$$

in equ. (2.2). Since θ appears only in the asymptotic expression (9.9), we have

$$\frac{\partial}{\partial\theta}\left\{\left(\frac{2k_o a}{\pi \sin\theta}\right)^{1/2} \exp\left[i\frac{3\pi}{4} - i\left(\nu+\frac{1}{2}\right)\theta\right]\right\} \tag{9.14}$$

$$\approx\left(\frac{2k_o a}{\pi \sin\theta}\right)^{1/2}\left[-ik_o a\right] \exp\left[i\frac{3\pi}{4} - i\left(\nu+\frac{1}{2}\right)\theta\right].$$

Using equ. (9.14), we obtain for the electric field E_ϕ,

$$E_\phi = \frac{Mk_o^{2/3}\omega\mu}{4\alpha^2 a^{1/3}\rho^{1/3}}\left(\frac{2k_o^2}{\pi \sin\theta}\right)^{1/2} e^{i\frac{3\pi}{4}} e^{-i\frac{1}{2}\theta} \cdot$$

$$\sum_\nu e^{i\frac{1}{2}k_o a\theta\lambda_\nu} \cdot \tag{9.15}$$

$$\frac{(h_1(0)h_2(h_0) - h_2(0)h_1(h_0))\ (h_1(0)h_2(h) - h_2(0)h_1(h))}{\left[1 - \frac{i}{\alpha(k_o a\rho)^{2/3}}\ k' h_1^2(0)\right]}$$

for $0 \leq h \leq h_1$.

It should be noted that the ratio U/U_0 does not differ appreciably from the ratio of electric fields $E_\phi/E_{\phi prm}$. As long as the distance R at which the field is measured is very much greater than a wavelength it is sufficient to use the ratio U/U_0.

It will be of interest in later calculations to compare the value of the potential U in a layered atmosphere with those values when no layer is present. For an homogenous troposphere we then have

$$\frac{U}{U_o} = \frac{\theta^{1/2} \; e^{-i\frac{1}{2}\theta}}{(\sin\theta)^{1/2}} \quad \frac{2\pi \; (k_o a)^{1/3} \theta^{1/2}}{\rho^{1/3}} \; e^{i\frac{3\pi}{4}} \; . \tag{9.16}$$

$$\sum_{\nu} e^{i\frac{1}{2} k_o a \theta \lambda_\nu} \frac{h_2(h_0)h_2(h)}{\left[h_2'(0)\right]^2}$$

where the λ_ν are roots of the equation

$$h_2 \left(\left(\frac{k_o}{a_1}\right)^{2/3} \lambda_\nu\right) = 0 \tag{9.17}$$

and

$$h_2(h_0) = h_2\left(\left(\frac{k_o}{a_1}\right)^{2/3} (y_0 + a_1 h_0 + \lambda_\nu)\right). \tag{9.18}$$

As a check on these results, it is of interest to compare the term in the denominator of equation (9.11), namely

$$1 - \frac{i}{\alpha (k_o a\rho)^{2/3}} \; k' h_1^2(\lambda_\nu) \tag{9.19}$$

with the result of Furry [16] for completely trapped modes. Here we have written $h_1(\lambda_\nu)$ instead of $h_1(0)$ to emphasize the fact that λ_ν is

complex. This factor is proportional to the normalization constant for the eigenfunctions, i.e., the solutions of equation (7.13). For this factor Furry gets, in terms of our notation

$$C_\nu^{-2} = \int_{h_{01}}^{h_{02}} (y(h) + \alpha_\nu)^{-1/2}\, dh - \left(\frac{k_o}{2\rho^2}\right)^{-1/3} \left(\frac{\alpha}{|h_1(\alpha_\nu)|^2}\right) \qquad (9.20)$$

where the eigenvalues λ_ν are written as

$$\lambda_\nu = \alpha_\nu + i\beta_\nu \ . \qquad (9.21)$$

Carrying out the integration, we get

$$C_\nu^{-2} = -\left(\frac{k_o}{\rho^2 a^2}\right)^{-1/3} \frac{\alpha^2}{|h_1(\alpha_\nu)|^2} \left\{1 - \frac{2k_o^{1/3}\left(\frac{a_2 - a_1}{a_1 a_2}\right)}{\alpha(\rho^2 a^2)^{1/3}} \right. \qquad (9.22)$$

$$\left. (y_1 + \alpha_\nu)^{1/2}/h_1(\alpha_\nu)^2 \right\} \ .$$

We will concentrate on the factor in large parenthesis. For completely trapped modes we obtain

$$k \simeq e^{i\pi/3}\, e^{-i\frac{4h_a}{3}\left(\frac{a_2 - a_1}{a_1 a_2}\right)[y_1 + \lambda_\nu]^{3/2}} \ . \qquad (9.23)$$

so that expression (9.19) becomes

$$1 - \frac{2h_a^{1/3}\left(\frac{a_1 - a_2}{a_1 a_2}\right)[y_1 + \lambda_\nu]^{1/2}}{\alpha(a\rho)^{2/3}} \cdot e^{+ i\frac{\pi}{3}} \cdot$$

$$e^{- i\frac{4k_o}{3}\left(\frac{a_2 - a_1}{a_1 a_2}\right)(y_1 + \lambda_\nu)^{3/2} h_1^{\,2}(\lambda_\nu)} \cdot \tag{9.24}$$

But at the eigenvalue for completely trapped modes (see Section 10.2)

$$\frac{2k_o}{3}\left(\frac{a_2 - a_1}{a_1 a_2}\right)(y_1 + \lambda_\nu)^{3/2} = (m - 1/2)\pi \qquad m = 1,2,3,... \tag{9.25}$$

Then expression (9.24) becomes

$$1 + \frac{2k_o^{1/3}\left(\frac{a_2 - a_1}{a_1 a_2}\right)(y_1 + \lambda_\nu)^{1/2}}{\alpha(a\rho)^{2/3}} \left(e^{i\pi/6} h_1(\lambda_\nu)^2\right) . \tag{9.26}$$

For the completely trapped modes $\lambda_\nu \cong \alpha_\nu$, to a high approximation. Furthermore, Furry introduces the correction factor δ so that

$$e^{i\pi/6} - i\delta\, h_1(\alpha_\nu) = \text{pure imaginary} . \tag{9.27}$$

Using this fact in equation (9.26) we obtain,

$$1 - \frac{2k_o^{1/3} \left(\frac{a_2 - a_1}{a_1 a_2}\right) (y_1 + \alpha_\nu)^{1/2}}{\alpha (a\rho)^{2/3}} \left| h_1(\alpha_\nu) \right|^2 \qquad (9.28)$$

which agrees with equation (9.22) for the term in brackets.

SECTION 10

NUMERICAL RESULTS

10.1 Description of the Computer Calculations

The computations were done in three major steps. First, the Hankel functions were calculated; second, the roots of the transcendental equation (7.21) were found and finally the Hertz potential function, essentially a sum of the roots, was obtained. In the expressions for the roots of the transcendental equation and the Hertz potential or electric field, Hankel functions of the first and second kind of order one-third and complex argument z, i.e., $H_{1/3}^{(1)(2)}(z)$, and their derivatives, appear. The variable z takes on the whole range of complex values, from very small to very large. To evaluate these functions, we made use of the Furry [16] infinite series and asymptotic series expressions for the modified Hankel functions of order one-third, $h_{(1)(2)}$ [see Appendix D and Section 10.2]. As our condition on the accuracy of the calculations, we required agreement with the tabulated results. This meant that the modified Hankel functions had to be calculated at least in double-precision (fourteen place accuracy) on the IBM 370-155*. (This was also the limitation of the present software available.) It turned out that the agreement of the calculated results with the tables was good to seven (out of eight) significant figures after the decimal point. This was satisfactory. The series expression for the Hankel functions were used for $|z| < 6$ and the asymptotic expressions for $|z| \geq 6$. The series in the asymptotic expressions was carried to powers in z of $z^{-21/2}$. The agreement between the two series at $z = 6$ is one-to-one. In the case of the asymptotic series one must be very careful so as to use the proper expressions in

*As an historical note, it is interesting to reflect that the tabulated results were obtained by the Harvard Computation Laboratory (now Aiken Computational Center) in 1944.

the various domains of the complex plane. In particular, if the magnitude of z is large, and z is very near the negative real axis, it is more convenient to use the Miller asymptotic formulas valid for $\frac{2\pi}{3} < \arg < \frac{4\pi}{3}$ [16] .

The next major task was the calculation of the roots of the transcendental equation (7.21). This turned out to be the most difficult and time consuming operation of the whole program. The problem was complicated not only by the fact that the roots were in the complex plane but also by the fact that roots of large real part and extremely small imaginary part (trapped modes) had to be obtained. The expression for the transcendental equation (7.21) can be written either as

$$F \equiv h_2(\lambda_\nu) - k(h_1,h_2,\lambda_\nu)\, h_1\,(\lambda_\nu) = 0 \tag{10.1}$$

or as

$$F \equiv \frac{h_2(\lambda_\nu)}{h_1(\lambda_\nu)} - k(h_1,h_2,\lambda_\nu) = 0 \tag{10.2}$$

To obtain the roots corresponding to the trapped modes it is essential to use the second form for F, since both h_2 and h_1 are very large simultaneously. The secant and the Newton-Raphson iteration methods [17] were used to solve F = 0 for λ_ν. The experience of previous investigators attempting to solve similar problems had been that the two methods give, in general, good convergence in the complex plane. Each method, however, was cited to give no convergence for particular geometries of F in the complex plane. The recommendation in those instances has been to go simply to another method. It would be presumptuous to make a general conclusion on which of the two methods gives more rapid convergence, for this depends on the particular problems involved; speaking only for our problem it was found that the Newton-Rhapson method gives somewhat better rate of convergence. The

roots found, however, by each method are identical for the same error bound on λ_ν, i.e., $|\lambda_\nu^{(n)} - \lambda_\nu^{(n-1)}| < \varepsilon$. The disadvantage of both methods is the requirement that the initial guess of a root must be fairly close to the actual location of that root to obtain convergence at all. The advantage of the secant method is that it involves only F whereas the Newton-Rhapson method involves the derivative of F, which in our problem is not a trivial calculation. Since we were guided by minimizing the computer running time, all roots presented in this report were found by the Newton-Rhapson method.

The calculation of the Hertz potential presented no special computational problems, and hence needs no further discussion. A more detailed description of the computational work described above, including computer flow charts, will appear in a companion report.

10.2 Calculation of the Characteristic Values for the Propagation Modes

The complex roots or characteristic values of the transcendental equation (7.21) can be thought of as propagation modes similar to those encountered in waveguide theory. However, the boundary value problem of the elevated duct is much more complicated than that since the elevated layer can not be simply modeled as a perfectly reflecting stratum. The modes that actually exist can be classified as "trapped" modes, "transitional" modes and "leaky" modes. This becomes clearer if we think of the geometric interpretation in Figure 10.1. The first trapped mode is m = 1 and the last is m = 5. There are always a finite number of these. In terms of the roots λ_ν of equ. (7.21),

$$\frac{h_2(\lambda_\nu)}{h_1(\lambda_\nu)} - k(\lambda_\nu) = 0 \quad . \tag{7.21}$$

This means that the imaginary part of λ_ν is extremely small and to a high approximation $\lambda_\nu = -y(h_1)$. Mode number m = 5, for example, is

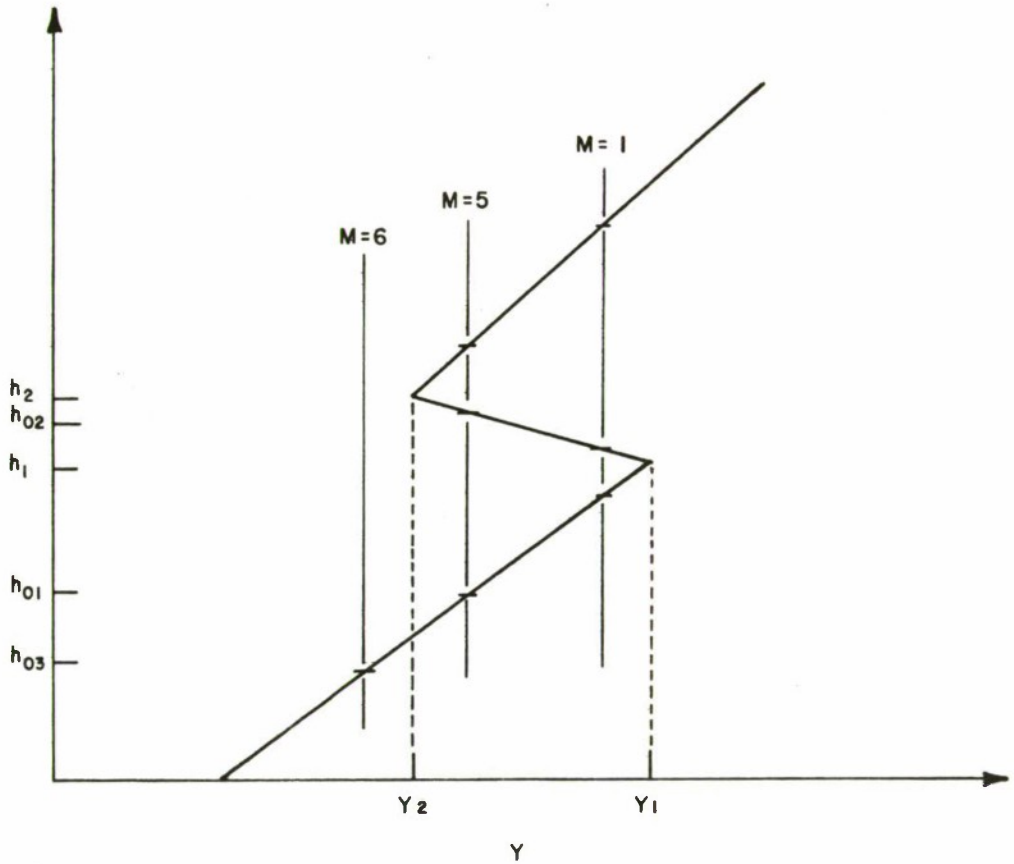

Figure 10.1 PROPAGATION MODES (EXAGGERATED DIMENSIONS)

confined essentially to the heights between h_1 and h_2 and is characterized by a very small variation of attenuation with range. When the imaginary part of λ_ν, $\mathrm{Im}(\lambda_\nu)$, is small and the real part $\mathrm{Re}(\lambda_\nu) \approx -y(h_2)$, we are said to have transitional modes, e.g., m = 6 in Figure 10.1. Physically these modes correspond to waves that just leak out of the duct. The characteristic values λ_ν, that have real parts comparable in magnitude to their imaginary parts are said to be leaky. These modes do not allow such a simple geometric interpretation as the previous two.

Now let us turn to the solution of equation (7.21) for λ_ν. We started by finding the roots corresponding to the trapped modes. But, as we pointed out in Section 10.1, for rapid convergence to a root by either the secant or the Newton-Rhapson iteration methods, it is essential that the initial guess of a root must be fairly close to the root itself. To get a handle on this problem we approximated the Hankel functions appearing in (7.21) by their asymptotic representations, keeping only the first terms. In this case $k(\lambda_\nu)$ is given approximately by

$$k \approx e^{i\frac{\pi}{3}} e^{-i\frac{4k_a}{3}\left(\frac{a_2 - a_1}{a_1 a_2}\right)[y_1 + \lambda_\nu]^{3/2}} \tag{10.3}$$

where the notation has been explained previously. And equation (7.21) becomes essentially

$$1 + e^{-iX} = 0 \tag{10.4}$$

where X is given by

$$X = \frac{4k_a}{3}\left(\frac{a_2 - a_1}{a_1 a_2}\right)[y_1 + \lambda_\nu]^{3/2} . \tag{10.5}$$

Equation (10.4) is satisfied for

$$X = m\pi \qquad (m \text{ is odd}). \tag{10.6}$$

As a check, we compared this result with the Furry-Gamow phase-integral method [4]. In this method the real part of λ_ν is determined by

$$k_a \int_{h_{01}}^{h_{02}} [y(h) + \lambda_\nu]^{1/2} \, dh = (m - \tfrac{1}{2})\,\pi \qquad m = 1,2,3.... \tag{10.7}$$

where the h_{01} and h_{02} satisfy $y(h) + \lambda_\nu = 0$. A straight-forward integration in two parts from h_{01} to h_1 and h_1 to h_{02} gives

$$\frac{2k_a}{3} \left(\frac{a_2 - a_1}{a_1 a_2}\right) [y_1 + \lambda_\nu]^{3/2} = (m - \tfrac{1}{2})\,\pi \qquad m = 1,2,3.... \; . \tag{10.8}$$

It is seen that the results are identical. Equation (10.7) is known as the "phase-integral condition". The cases for which this method applies are as follows:

(i) The curve $y(h)$ must have at least one minimum, in our case it has two, $y(h_1)$ and $y(h_2)$; a mode to which the method can be applied must have

$$-y(h_1) < \mathrm{Re}(\lambda_\nu) < -y(h_2) \tag{10.9}$$

so that the waves are trapped; and it must have

$$\begin{aligned} \mathrm{Im}(\lambda_\nu) &\ll -(y(h_1) + \mathrm{Re}(\lambda_\nu)) \\ \mathrm{Im}(\lambda_\nu) &\ll -(y(h_2) + \mathrm{Re}(\lambda_\nu)) \; ; \end{aligned} \tag{10.10}$$

(ii) The value of $\mathrm{Re}(\lambda_\nu)$ is found from equ. (10.8). After the $\mathrm{Re}(\lambda_\nu)$ is known, $\mathrm{Im}(\lambda_\nu)$ is calculated from an explicit real expression to be derived presently.

For the determination of the imaginary part of λ_ν we will use the modified index of refraction profile y(h) of equ. (8.1), Figure 8.2. Let us write the characteristic values λ_ν as

$$\lambda_\nu = \alpha_\nu + i\beta_\nu \quad . \tag{10.11}$$

We will now extend the formulas Furry [3] derived for a single minimum of y(h) to two minima. The imaginary part β_ν is then given by (see Figure 10.2)

$$\beta_\nu = C_\nu^{\,2}\, k_a^{-1}\, e^{-2 W_\nu} \tag{10.12}$$

where

$$C_\nu^{-2} \approx 2 \int_{h_{01}}^{h_{02}} (y(h) + \alpha_\nu)^{1/2} \, dh \tag{10.13}$$

$$W_m = k_a \int_{h_{02}}^{h_{03}} |y(h) - \alpha_\nu|^{1/2} \, dh \tag{10.14}$$

and $k_a = 2\pi/\lambda$, where λ is the wavelength. When equs. (10.18) and (10.14) are applied to the profile of Figure 10.2 we obtain

$$C_\nu^{-2} = 4\, (y_1 + \alpha_\nu)^{1/2} \left(\frac{a_2 - a_1}{a_1 a_2}\right) \tag{10.15}$$

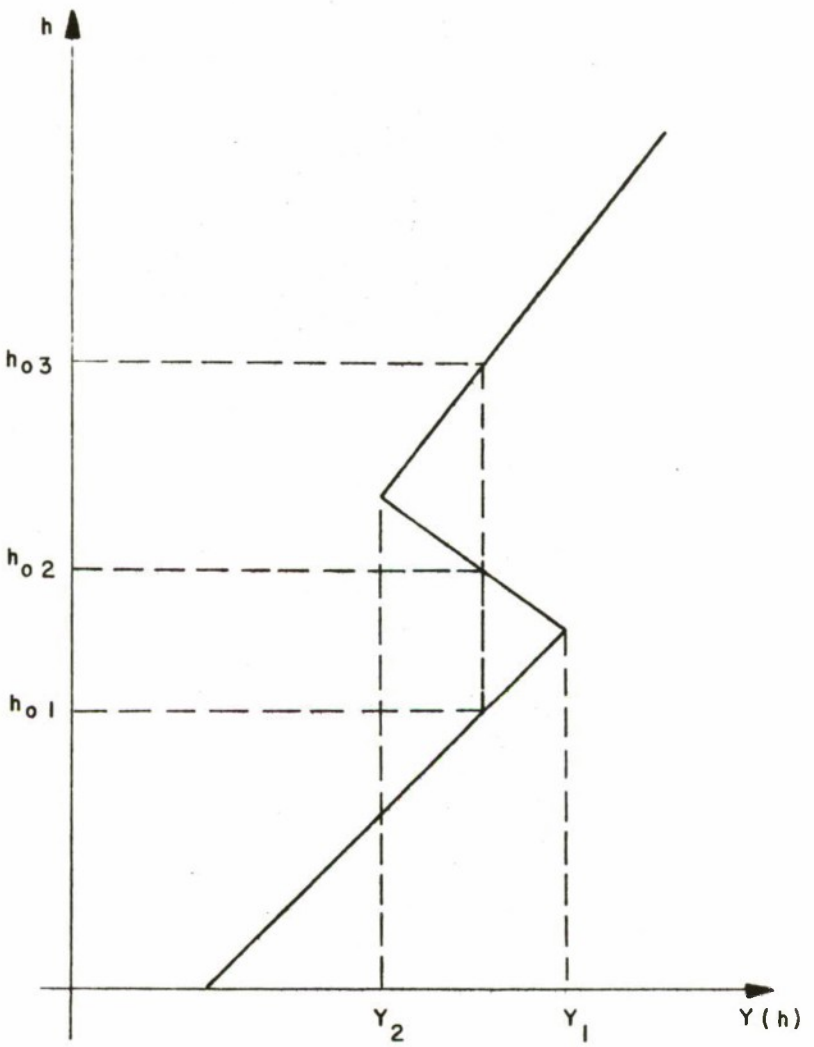

IA-37,506

Figure 10.2 Y (h) PROFILE

and

$$W_m = \frac{2k_a}{3} (-y_2 - \alpha_\nu)^{3/2} \left(\frac{a_2 - a_1}{a_1 a_2}\right) . \tag{10.16}$$

The α_ν are determined from equ. (10.6) or (10.8). For later comparison we shall call these α_ν, β_ν the Furry-Gamow roots. It is seen from equ. (10.16) that the condition (10.10) requires

$$e^{-2 W_m} << 1$$

and (10.17)

$$C_\nu^2 << 1 .$$

This implies that the values of β_ν will be in error near $\alpha_\nu = -y_1$ and $\alpha_\nu = -y_2$. It is surprising, however, how good these approximate values of α_ν and β_ν are to the exact values determined by the Newton-Rhapson method. As a particular example we have chosen the following constraints:

$$\lambda = 1 \text{ meter}$$

$$y_1 = 211.66 \times 10^{-6}$$

$$y_2 = 131.66 \times 10^{-6}$$

$$a_1 = 2.3518 \times 10^{-7}$$

$$a_2 = -8.0 \times 10^{-7}$$

In Table 10.1 are shown the Furry-Gamow roots and their exact values. From these results it is seen that the real part of λ_ν is in error by less than one percent. The imaginary part of λ_ν is in error by about 10%; except for m = 2 where the error is about 30%. The 10% error can be explained from the fact that condition (10.17) is not always satisfied. There is no ready explanation for the 30% error in mode number 2.

Mode Number m	Furry - Gamow (λ_ν)	Exact (λ_ν)
1	$-194.98 \times 10^{-6} + i0.1434 \times 10^{-15}$	$-195.84 \times 10^{-6} + i0.1285 \times 10^{-15}$
2	$-176.85 \times 10^{-6} + i0.1009 \times 10^{-11}$	$-177.44 \times 10^{-6} + i0.0773 \times 10^{-11}$
3	$-162.87 \times 10^{-6} + i0.3334 \times 10^{-9}$	$-162.88 \times 10^{-6} + i0.3234 \times 10^{-9}$
4	$-150.6 \times 10^{-6} + i0.2068 \times 10^{-7}$	$-150.64 \times 10^{-6} + i0.2268 \times 10^{-7}$
5	$-139.46 \times 10^{-6} + i0.3117 \times 10^{-6}$	$-140.02 \times 10^{-6} + i0.3244 \times 10^{-6}$

TABLE 10.1 COMPARISON OF FURRY-GAMOW ROOTS AND EXACT ROOTS

It can be concluded, however, that the Furry-Gamow values serve as an excellent guide for the initial guess of a root and for this reason alone are indispensible.

There are no such relatively simple formulas that give the roots corresponding to the transitional and leaky modes. It was fortuitous that the location of these roots could be predicted reasonably accurately by linear extrapolation from the trapped mode root values. However, in only one instance could the location of three successive roots be predicted by linear extrapolation. The reason for this failure can be seen from the non-linear character of β_ν as a function of mode number in Figure 10.3. It is perhaps advantages to use some curve fitting routine to predict more root values in advance; this was not tried here. Such a procedure would certainly cut down on the computer running time if it proves successful.

There was another way in which we went about locating a root for a particular set of values of the parameters λ, y_1, y_2, a_1 and a_2. This approach was motivated by Northover's [18] investigation in which he considered reflections from an elevated layer by treating such a layer as a discontinuity in the index of refraction. He predicted that for the important modes in ground to ground communications, namely those waves that are reflected by the elevated layer back to the receiver should have corresponding characteristic values whose magnitude is less than unity. In terms of our notation this condition means that

$$\left| \left(\frac{k_o}{a_1} \right)^{2/3} \lambda_\nu \right| < 1 . \qquad (10.18)$$

They correspond to leaky modes. It turned out that these roots could be found rather quickly since there were always just a few of them (see e.g., Table 10.2). And the real and imaginary parts were of comparable magnitude. These roots then provided another starting point

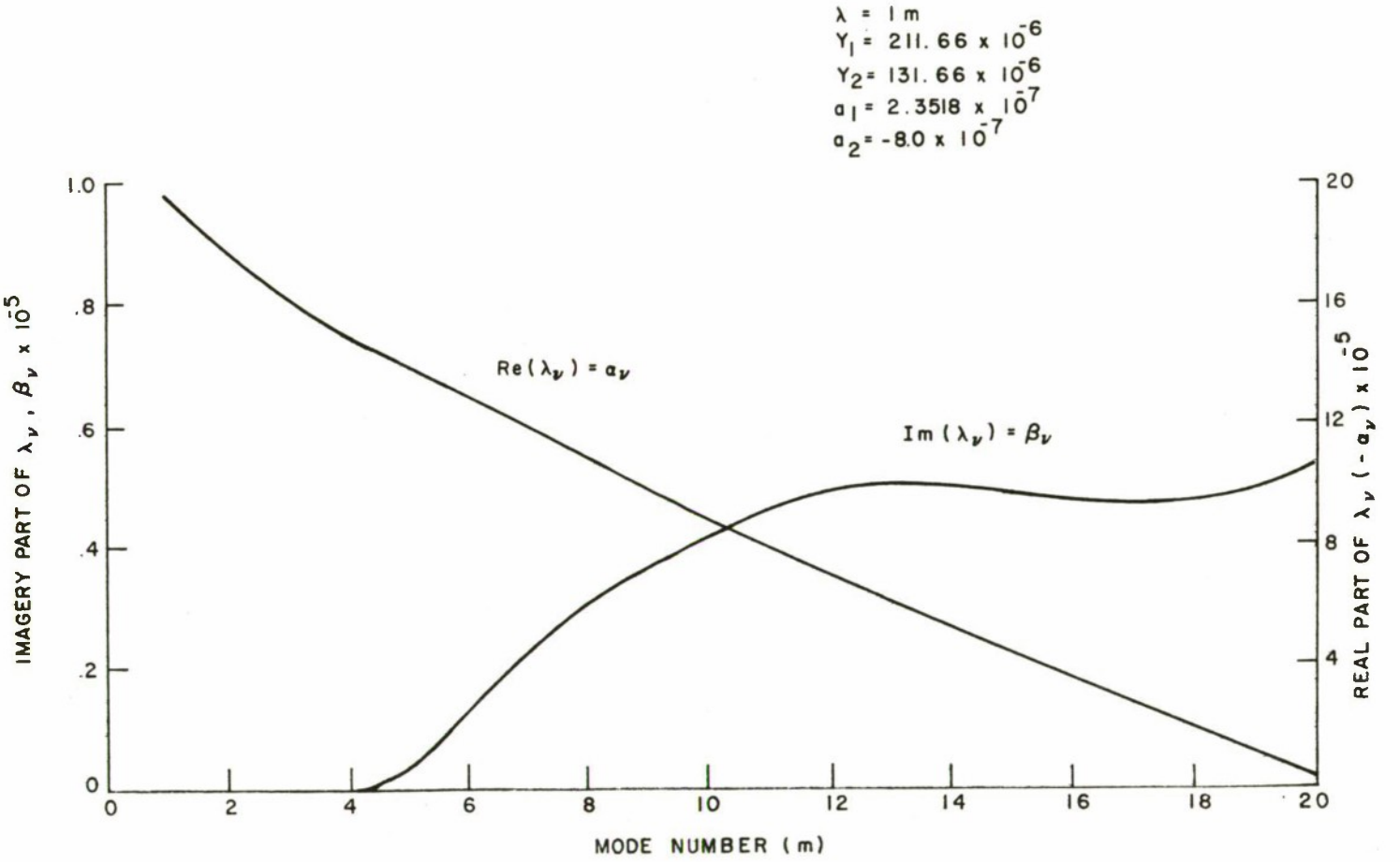

Figure 10.3 CHARACTERISTIC VALUES AS A FUNCTION OF MODE NUMBER

for finding additional characteristic values. This procedure proved to be very convenient.

10.3 Discussion of the Characteristic Values and Their Physical Interpretation

All the characteristic values, λ_ν, we have found are listed in Tables 10.2, 10.3 and 10.4. The accuracy of these values obtained on the computer was actually 14 places; they have been rounded off to five places after the decimal in the tables. The values were obtained as a function of frequency (wavelength λ), and layer height, h_i, as a function of lapse rate within the layer, a_2 and outside the layer, a_1 and as a function of the value of y(h) at the start of the layer, y_1 and at its termination y_2.

The real part of the characteristic values enters as a phase factor in the final expression for the field, equ. (9.15). Each characteristic value or mode is seen to have a different phase and hence, the addition of many such modes results in appropriate phase vector addition. The imaginary part of λ_ν corresponds to the attenuation of the mode. This can be written as

$$\text{attenuation} = \frac{e^{1/2\ \beta_\nu k_o d}}{\sqrt{d}} \tag{10.19}$$

It is seen from the tables that the trapped modes have a very small imaginary part so that the attenuation of these is like $(1/\sqrt{d})$. It is noted from a comparison of Tables 10.2 and 10.3 that the thicker layer (100 meters) has the smaller imaginary part for the first mode, hence the attenuation of this mode is smaller. It will be seen in Section 10.4 that this will also correspond to more energy being trapped in the duct. In both cases the first five modes are trapped. In Table 10.4, the layer is even thicker (150 m) but we have lowered the frequency to 150 MHz and as a result the first mode has an imaginary part several orders of magnitude greater than for 300 MHz. In addition,

Mode Number	Characteristic Values	
m	Real Part ($\times 10^{-5}$)	Imaginary Part
1	-19.25747	$.31597 \times 10^{-13}$
2	-17.33864	$.56905 \times 10^{-10}$
3	-15.78268	$.77958 \times 10^{-8}$
4	-14.43457	$.17336 \times 10^{-6}$
5	-13.20194	$.84462 \times 10^{-6}$
6	-12.00625	$.16483 \times 10^{-5}$
7	-10.85324	$.22246 \times 10^{-5}$
8	- 9.75080	$.26214 \times 10^{-5}$
9	- 8.69502	$.29129 \times 10^{-5}$
10	- 7.68003	$.31404 \times 10^{-5}$
11	- 6.70058	$.33267 \times 10^{-5}$
12	- 5.75236	$.34849 \times 10^{-5}$
13	- 4.83184	$.36233 \times 10^{-5}$
14	- 3.93611	$.37476 \times 10^{-5}$
15	- 3.06264	$.38639 \times 10^{-5}$
16	- 2.21008	$.42040 \times 10^{-5}$
17	- 1.36162	$.42117 \times 10^{-5}$
18	- .49410	$.46243 \times 10^{-5}$
19	.43138	$.52265 \times 10^{-5}$
20	1.43287	$.59324 \times 10^{-5}$
21	2.51086	$.66949 \times 10^{-5}$
22	3.66053	$.75062 \times 10^{-5}$
23	4.87641	$.83685 \times 10^{-5}$
24	6.15302	$.92792 \times 10^{-5}$
25	7.48485	1.02197×10^{-5}
26	8.86721	1.11422×10^{-5}
27	10.29907	1.19673×10^{-5}
28	11.78600	1.26204×10^{-5}
29	13.33784	1.30910×10^{-5}
30	14.96139	1.34344×10^{-5}

TABLE 10.2 CHARACTERISTIC VALUES
(λ = 1m, ΔM = 40 in 30m, h_i = 900m)

Mode Number	Characteristic Values	
m	Real Part ($\times 10^{-5}$)	Imaginary Part
1	-19.58371	$.12851 \times 10^{-15}$
2	-17.74367	$.77288 \times 10^{-12}$
3	-16.28801	$.32337 \times 10^{-9}$
4	-15.06395	$.22680 \times 10^{-7}$
5	-14.00183	$.32445 \times 10^{-6}$
6	-12.98671	$.12363 \times 10^{-5}$
7	-11.94416	$.22376 \times 10^{-5}$
8	-10.90414	$.30204 \times 10^{-5}$
9	- 9.89299	$.36548 \times 10^{-5}$
10	- 8.91984	$.41982 \times 10^{-5}$
11	- 7.98680	$.46395 \times 10^{-5}$
12	- 7.08954	$.49208 \times 10^{-5}$
13	- 6.21641	$.50117 \times 10^{-5}$
14	- 5.35600	$.49691 \times 10^{-5}$
15	- 4.50455	$.48825 \times 10^{-5}$
16	- 3.66337	$.48082 \times 10^{-5}$
17	- 2.83430	$.47709 \times 10^{-5}$
18	- 2.01671	$.48026 \times 10^{-5}$
19	- 1.20037	$.49915 \times 10^{-5}$
20	- .35700	$.54292 \times 10^{-5}$
21	.54346	$.60849 \times 10^{-5}$
22	1.51098	$.68840 \times 10^{-5}$
23	2.53954	$.77999 \times 10^{-5}$
24	3.61628	$.88048 \times 10^{-5}$
25	4.72710	$.97651 \times 10^{-5}$
26	5.87686	1.04212×10^{-5}
27	7.09619	1.07111×10^{-5}
28	8.40164	1.08675×10^{-5}

TABLE 10.3 CHARACTERISTIC VALUES
(λ = 1m, ΔM = 40 in 100m, h_i = 900m)

Mode Number	Characteristic Values	
m	Real Part ($\times 10^{-5}$)	Imaginary Part
1	-40.04153	$.55272 \times 10^{-10}$
2	-37.25141	$.31514 \times 10^{-7}$
3	-35.18809	$.93090 \times 10^{-6}$
4	-33.36697	$.36497 \times 10^{-5}$
5	-31.49586	$.56410 \times 10^{-5}$
6	-29.63776	$.66557 \times 10^{-5}$

TABLE 10.4 CHARACTERISTIC VALUES
(λ = 2m, ΔM = 40 in 150m, h_i = 1800m)

only the first three modes are trapped resulting in lower signal strength within the duct.

10.4 Comparison of Calculated and Experimental Results

The calculations of field intensity relative to free-space were performed using expressions (9.11) and (9.12). The results are plotted in Figures 10.4 to 10.8. All curves are for a frequency of 300 MHz, and a layer height of 900 m. Two values of layer thickness, 30 m and 100 m, but of the same decrement in modified index of refraction, $\Delta M = 40$, have been used. Such layer values are representative of those measured in the trade winds ducts near San Diego, Calif. [19] and the South Atlantic [20]. The field intensity is plotted as a function of height and distance for various transmitter locations. A comparison of the plots shows that the thicker layer (100 meters) has also the greater field intensity values; a difference of about 10 dB on the average exists for the two layer thickness values. This appears logical since, for the same decrement ($\Delta M = 40$) the 100 meter layer results in a wider duct than the 30 meter layer and, hence, is capable of trapping more energy. When the transmitter is moved out of the duct, Figure 10.6, the field intensity decreases by approximately 5 dB on the average. In addition, we notice in this case interference between the waves that move above and are coupled into the layer and those that go through the duct strike the earth and then escape into the space above the layer. In Figure 10.6, constructive and destructive interference are observed at approximately 450 km and 500 km, respectively. The field intensity is given as a function of height in Figures 10.7 and 10.8. Here again, the wider duct results in a higher field strength, about 10 dB. We also notice in Figure 10.7 that we obtain interference type (multipath) lobing; the intensity of which decreases as one gets closer to the bottom of the layer. Furthermore, the field strength increases by approximately 5 dB from near the bottom of the duct to the top. This latter behavior does not appear to be in evidence for the wider duct in Figure 10.8.

IA-37,507

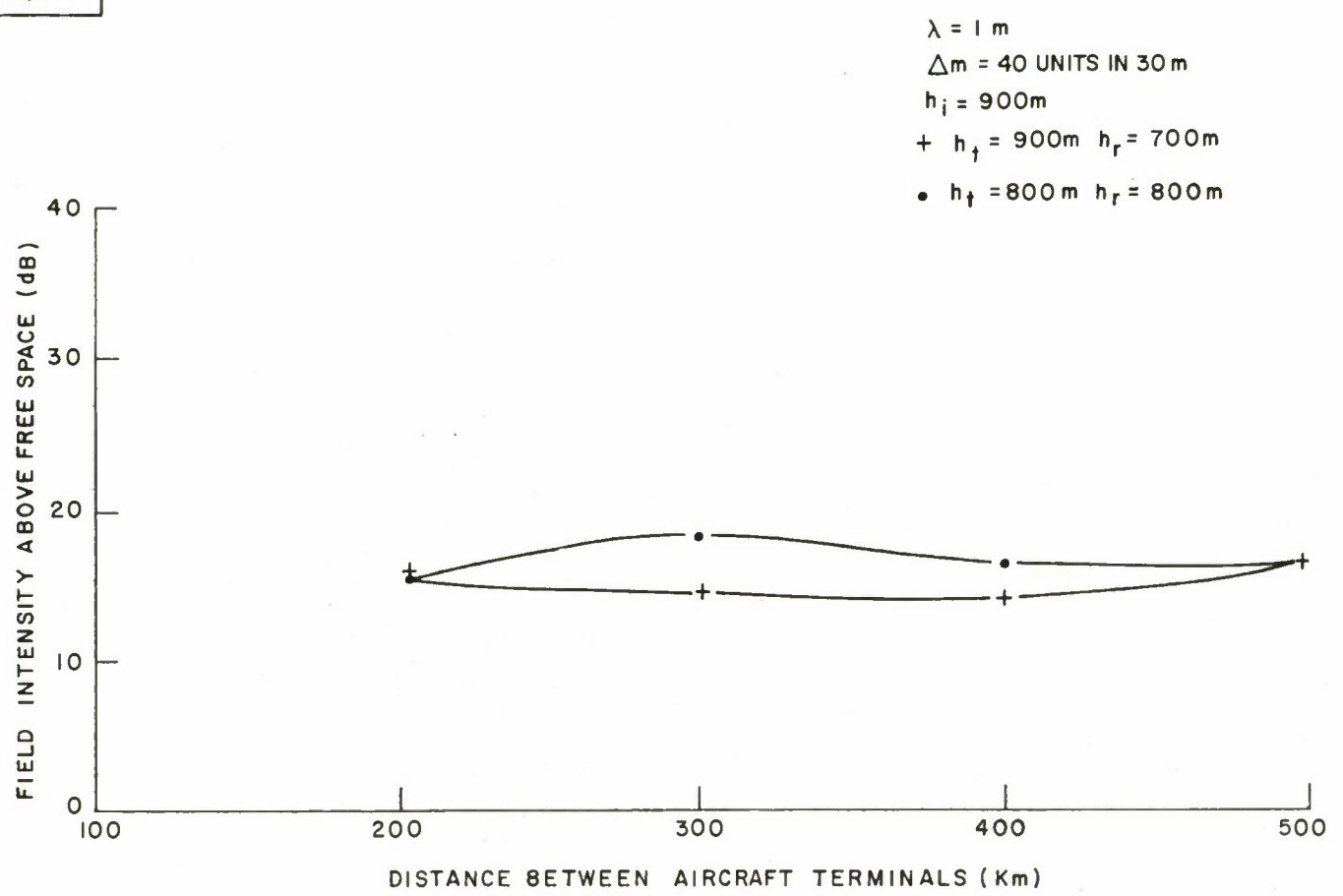

Figure 10.4 FIELD INTENSITY AS A FUNCTION OF TERMINAL SEPARATION (ΔM = 40 IN 30m)

IA-37,508

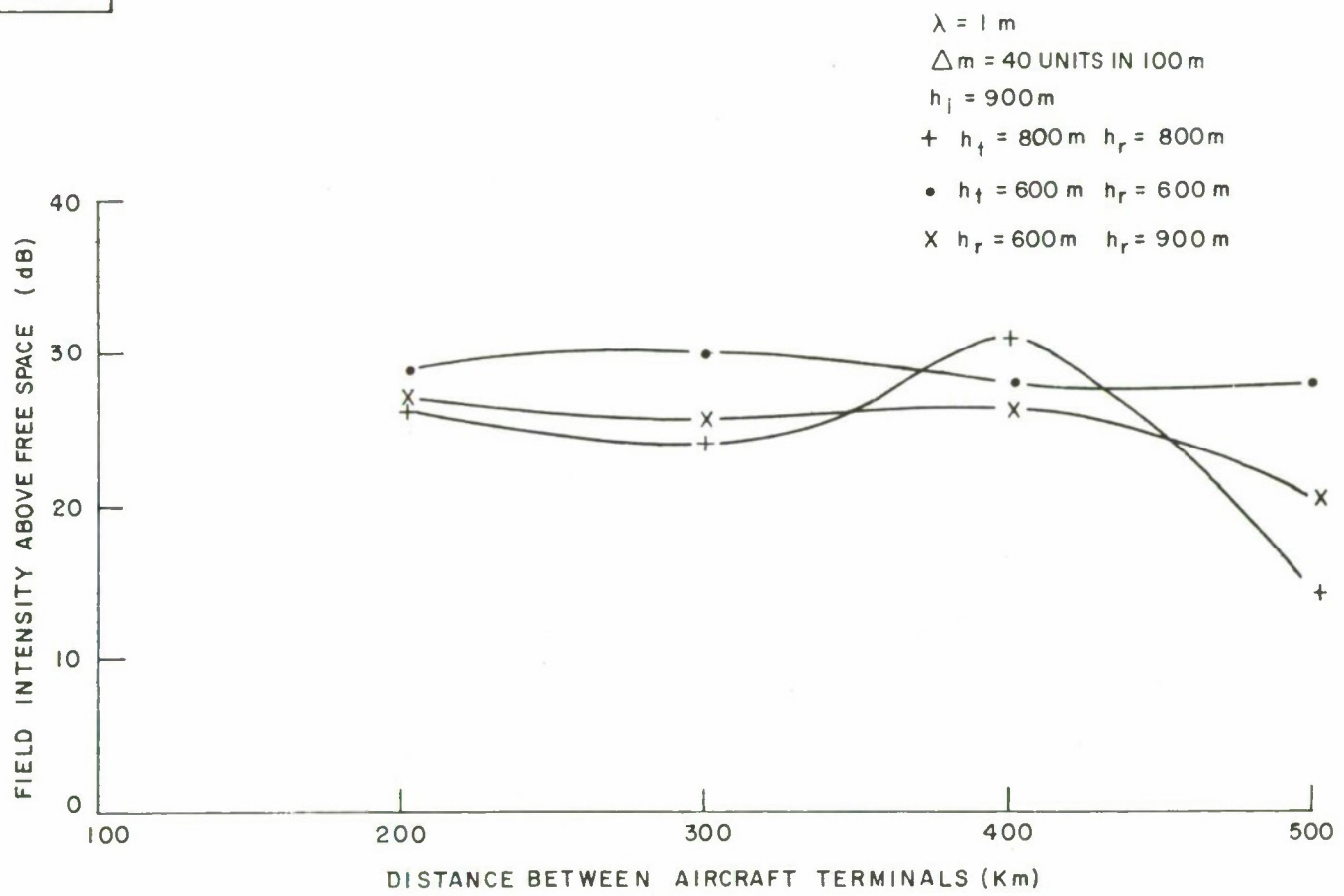

Figure 10.5 FIELD INTENSITY AS A FUNCTION OF TERMINAL SEPARATION (ΔM = 40 IN 100 m)

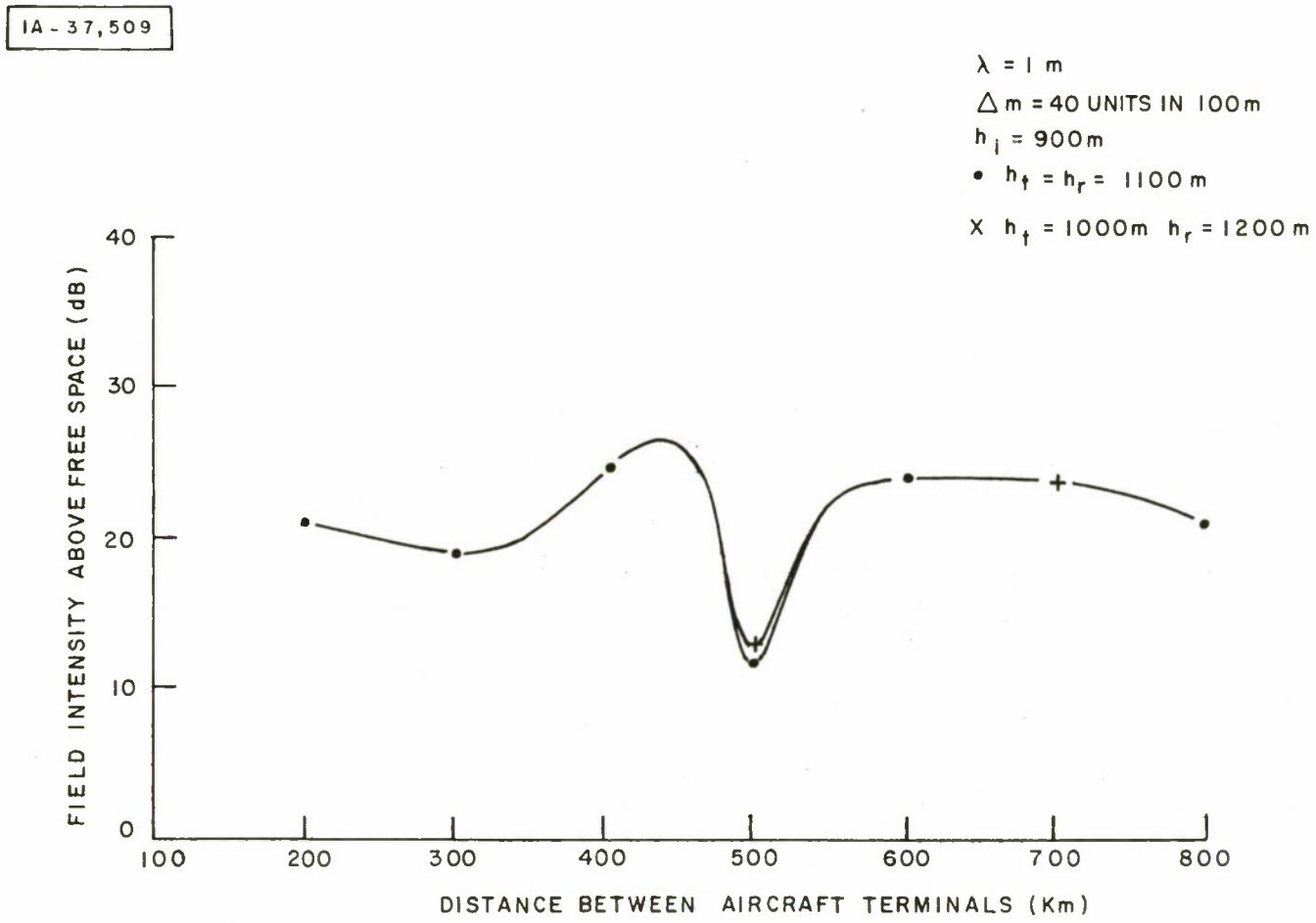

Figure 10.6 FIELD INTENSITY AS A FUNCTION OF TERMINAL SEPARATION (ΔM = 40 IN 100m)

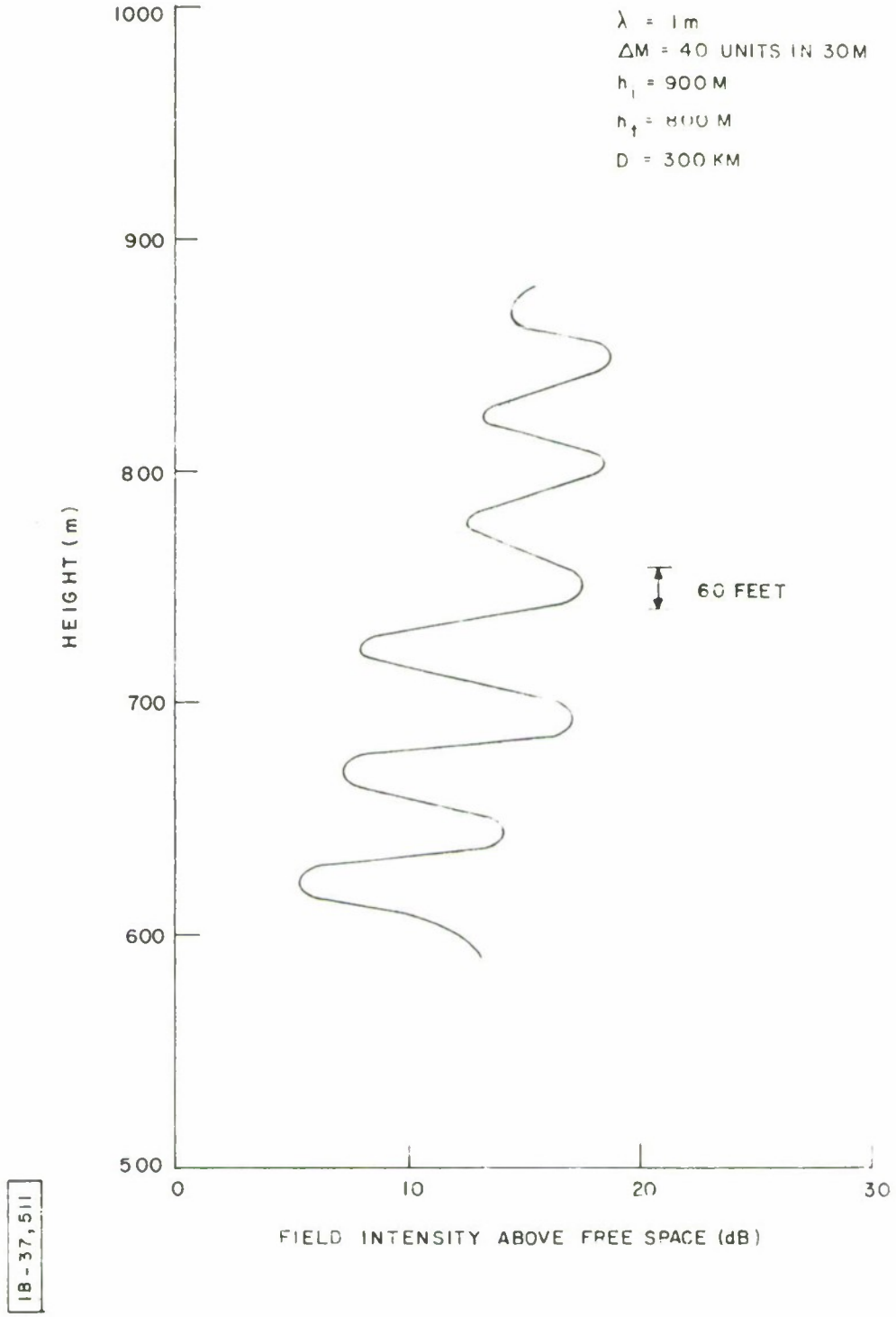

Figure 10.7. FIELD INTENSITY AS A FUNCTION OF HEIGHT
(Δm = 40 IN 30m)

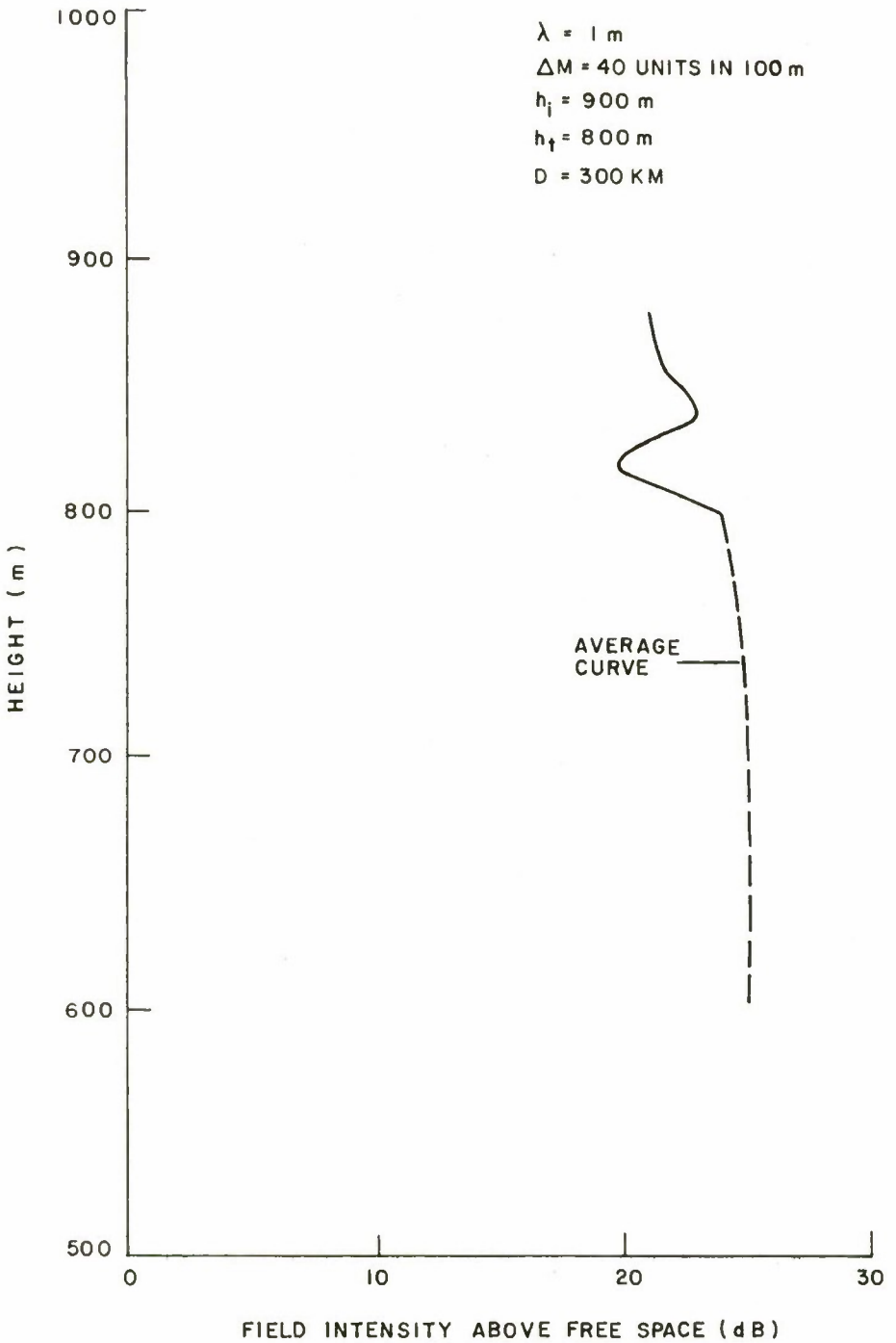

IB-37,512

Figure 10.8. FIELD INTENSITY AS A FUNCTION OF HEIGHT (ΔM = 40 IN 100 m)

We will now compare these results with some experimental evidence. For comparison, we use the test results of Project Neptune [21]. This project involved air-to-air and air-to-ground propagation testing in the trade wind ducts at 220 MHz. Its purpose was to explore the communication potentialities of the trade winds inversion layers. For comparison we will choose the thinner layer (30 m). It is to be noted that in these test results, the measured values of refractive index values are open to question [21]. The agreement between our results and the tests is good on a relative basis. When the results are compared on an absolute basis our results are approximately 10 - 15 dB higher. To partially explain this difference, we note that our results are for a somewhat higher frequency, 300 MHz versus 220 MHz. In general, the higher the frequency, the greater the extent of trapping, and hence, the higher signal level. Another difference is due to the fact that in our model the duct width and ΔM scenarios constant whereas in the tests the width and decrement actually changed in the distance. This would also increase the leakage from the duct and result in a lower signal level. In the tests it was observed that signal level increased from 5 to 20 dB as the receiver moved closer to the bottom of the layer. The field being highest at the base of the inversion. These results agree essentially with ours. We obtain an increase in signal level of 5 to 10 dB. Furthermore, it was reported that the signal level remained "relatively high" above the duct. This also agrees with our calculated results. It being that the signal is only approximately 5 dB less above the duct. Finally, the tests established good signal correlation for 60 feet ($\approx$18 m) vertically. If this result is compared with Figure 10.7, it is seen that it agrees quite well with the calculated numbers; our results showing about 80 feet at the 3 dB points.

SECTION 11

SUMMARY OF CURRENT RESULTS AND RECOMMENDATIONS FOR FUTURE WORK

We will here summarize the results we have obtained and explain their significance. Also, we will make several recommendations for future work. In addition, we will point out the most significant elements to be incorporated in a propagation experiment.

We have shown that the presence of elevated ducts can produce significantly higher signal strengths; on the order of 20 dB above free space. We have further demonstrated that the tri-linear model for the index of refraction is plausible and gives good agreement with experimental results on a relative basis but tends to make rather high estimates of signal strength on an absolute scale. We have shown the existence of interference type lobing at the duct height with 5 dB to 10 dB fades at 300 MHz and good signal correlation for vertical distances of roughly 80 feet. From an operational point of view, it is best to fly the transmitter and receiver at the base of the elevated layer. At this location signal strength is highest and interference type lobing is least. In order to avoid the 10 dB fades it is essential that space diversity reception be employed.

In the present report we have limited our analysis to the detailed analysis of a single frequency, 300 MHz. Future work should be extended to a comprehensive comparison of several frequencies. Spatial correlation distances of the signals should be obtained for such frequencies in order to obtain estimates of vertical and horizontal antenna diversity distances. Furthermore, a spectral analysis should be performed to estimate the signalling bandwidth that can be supported in the presence of elevated layers. And finally, the calculated results that have been obtained for heights within the duct and slightly above it should be extended to include the whole range from the ground to great heights.

From the above discussion it becomes quite clear what the most essential elements of any air-to-air propagation experiment should be. The most detrimental effect of this channel is interference type lobing. Hence, the experiment must, first, establish the signalling bandwidth it can support. This could be performed by probing the channel with a multi-tone signal consisting of a group of equally spaced frequencies. Secondly, the experiment must test some antenna diversity system in order to reduce the amplitude modulation caused by fading. A general experiment incorporating these elements is described in Reference 1.

APPENDIX A

JUSTIFICATION FOR THE HERTZ POTENTIAL

We shall show here that the one dimensional Hertz vector $\overline{\Pi} = (0,0,U)$ is a satisfactory approximation to the solution of Maxwell's equations.

Let us consider $\overline{\Pi}$ which satisfies the equation

$$\nabla \cdot \nabla \cdot \overline{\Pi} - \nabla\nabla \cdot \overline{\Pi} - \mu\varepsilon\omega^2 \overline{\Pi} = 0 \tag{A-1}$$

and construct the field vectors corresponding to the magnetic type (magnetic dipole), then

$$\overline{D} = - i\mu\varepsilon\omega\nabla \cdot \overline{\Pi} \tag{A-2}$$

$$\overline{H} = \nabla \cdot \nabla \cdot \overline{\Pi} \tag{A-3}$$

The vectors $\overline{D}$ and $\overline{H}$ satisfy the equations

$$\nabla \times \overline{E} = - i\omega\mu \overline{H} + \frac{\nabla\mu}{\mu} \times \overline{E} \tag{A-4}$$

$$\nabla \times \overline{H} = i\omega\varepsilon \overline{E} \tag{A-5}$$

$$\nabla \cdot \overline{D} = 0 \tag{A-6}$$

$$\nabla \cdot \overline{B} = \nabla\mu \cdot \overline{H} \quad . \tag{A-7}$$

It is seen that equations (A-4) to (A-7) do not satisfy Maxwell's equations exactly. For the atmosphere, however, the gradient of μ is extremely small so that terms involving it can be neglected. The

ratio of the magnitude of the second term to the first term on the right hand side of equ. (A-4) can be written as

$$\frac{\lambda}{2\pi} \frac{|\nabla\mu|}{\mu} \cdot \frac{\sqrt{\mu_0\varepsilon_0}}{\mu} \frac{|\overline{E}|}{|\overline{H}|} \quad . \tag{A-8}$$

Except quite close to the source, the field will be almost a plane wave for which $|\overline{E}|/|\overline{H}|$ is approximately $\sqrt{\mu/\varepsilon}$. Furthermore, $|\nabla\mu|/\mu$ is of the order of 10^{-5}, and therefore the ratio of the second term to the first term is of the order $\lambda \cdot 10^{-5}$, which is always very small compared to unity. From equs. (A-5) and (A-7) it follows that

$$\frac{\nabla \cdot \overline{B}}{|\nabla \cdot \overline{B}|} \approx \frac{\lambda}{2\pi} \frac{|\nabla\mu|}{\mu} \frac{\sqrt{\mu_0\varepsilon_0}}{\varepsilon} \frac{|\overline{H}|}{|\overline{E}|} \tag{A-9}$$

and this again is of the order of $\lambda \cdot 10^{-5}$. It follows that equs. (A-4) to (A-7) differ from MAxwell's equations by a negligible amount, and we may regard equations (A-2) and (A-3) as a valid way to obtain the electromagnetic field.

Because the Hertz vector has only its radial component non-zero, it follows that [19]

$$\nabla(\mu\varepsilon) \cdot \nabla \cdot \overline{\Pi} = 0 \quad \text{and} \quad \nabla(\mu\varepsilon) \cdot \overline{\Pi} = 0 \quad . \tag{A-10}$$

APPENDIX B

CONTOUR INTEGRAL REPRESENTATION FOR $U(r,\theta)$

Following a method due to Watson, we shall show that the series expression for $U(r,\theta)$, (3.9) can be expressed as a contour integral. Consider the series

$$S = \sum_{n=0}^{\infty} (2n + 1)\, f(n)\, P_n (\cos \theta) \tag{B.1}$$

where $f(n)$ is an analytic function of n. We will show that S can be represented by the following contour integral:

$$I = \int_C \frac{s}{i \cos \pi s} f\left(s - \frac{1}{2}\right) P_{s - 1/2} (\cos (\pi - \theta)) \tag{B.2}$$

where $C = C_1 + C_2$ is a contour that starts at $\infty - i\delta$ in the complex s-plane, goes below the real axis at $s = 0$ and then above the real axis to $\infty + i\delta$. Since $f(s - \frac{1}{2})$ and $P_{s - 1/2} (\cos (\pi - \theta))$ are analytic functions of s, the only singularities of the integral are poles at those values of s inside C for which $\cos \pi s = 0$, that is $s = 1/2, 3/2, 5/2, \ldots$

Equation (B.2) can be written as the sum over C_1 and C_2. Hence,

$$F = \int_{C_1} H(s)\, ds + \int_{C_2} H(s)\, ds \tag{B.3}$$

where $H(s)$ is the integrand in (B.2). In the second integral of (B.3) replace s by $-s$. This transformation reflects the contour C_2 about the origin into the contour C_3, as well as alters the integrand.

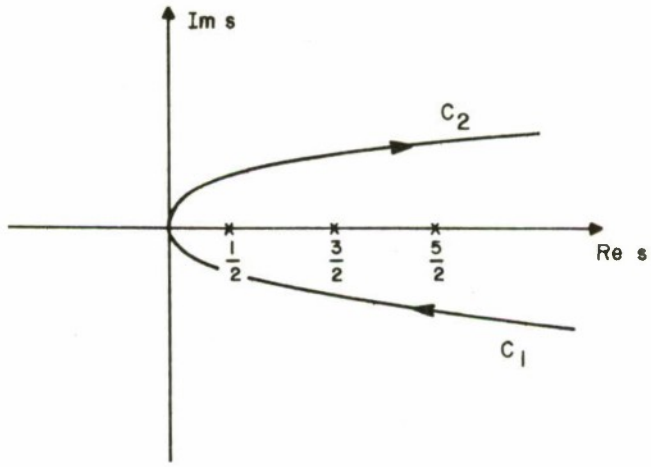

Figure B-1. COMPLEX S-PLANE

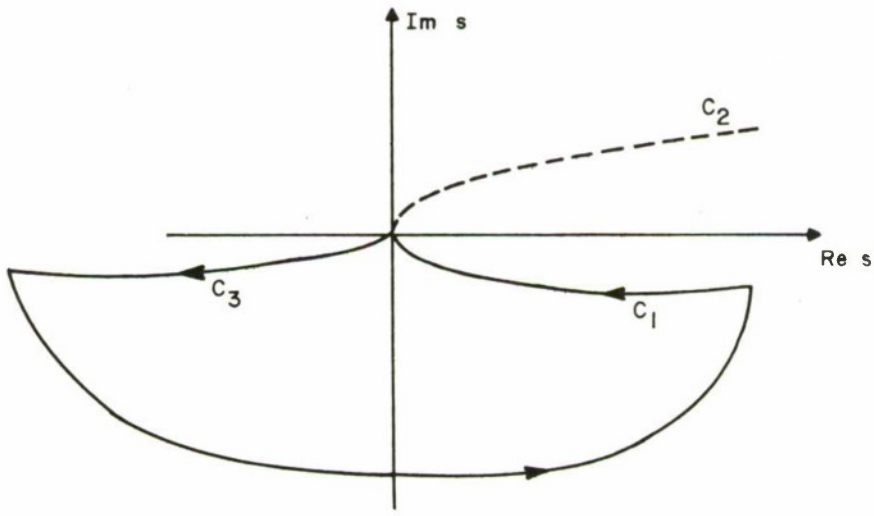

Figure B-2. TRANSFORMED PATH OF INTEGRATION

IA-37,816

Hence, equation (B.3) becomes

$$F = -\int_{C_3} H(-s)ds + \int_{C_1} H(s)ds \tag{B.4}$$

Adding and subtracting $\int_{C_2} H(s)ds$ to (B.4) results in

$$F = \int_{C_1 + C_3} H(s)ds - \int_{C_3} [H(s) + H(-s)]\, ds \ . \tag{B.5}$$

Using the fact that

$$P_{s - 1/2}(\cos(\pi - \theta)) = P_{-s - 1/2}(\cos(\pi - \theta)) \tag{B.6}$$

and substituting for H(s) we obtain

$$F = \int_{C_1 + C_3} \frac{s}{i \cos(\pi s)} f(s - \tfrac{1}{2})\, P_{s - 1/2}(\cos(\pi - \theta))\, ds$$

$$+ \int_{C_3} \frac{s}{i \cos \pi s} \left[f(-s - \tfrac{1}{2}) - f(s - \tfrac{1}{2}) \right] ds \ . \tag{B.7}$$

The contour $C_1 + C_3$ may be closed by a semicircle of infinite radius in the lower half plane as shown in Figure (B.2). Thus (B.7) becomes

$$F = \oint_{C_1+C_3+C_4} \left[\frac{s}{i \cos \pi s} f(s - \tfrac{1}{2}) P_{s-1/2}(\cos(\pi - \theta)) \right] ds + I_1 \qquad (B.8)$$

where I_1 is the second integral in (B.7).

Now substituting the expression for f obtained in the previous section,

$$f(s - \tfrac{1}{2}) = \frac{-M}{4\pi W_{s-1/2}} \begin{cases} Q_{s-1/2}(b)\, V_{s-1/2}(r) & r \leq b \\ V_{s-1/2}(b)\, Q_{s-1/2}(r) & r \geq b \end{cases} \qquad (B.9)$$

where $Q_{s-1/2}(r)$ and $V_{s-1/2}(r)$ represent analytic functions along the positive real axis. Substituting (5.9) into the expression for $U(r,\theta)$ we obtain

$$U(r,\theta) = \frac{-M}{4\pi i} \oint_{C_1+C_3+C_4} \frac{sds}{\cos \pi s} \frac{P_{s-1/2}}{W_{s-1/2}} \begin{cases} Q_{s-1/2}(b)\, V_{s-1/2}(r) & r \leq b \\ V_{s-1/2}(b)\, Q_{s-1/2}(r) & r \geq b . \end{cases} \qquad (B.10)$$

And if we replace s by $\nu + \frac{1}{2}$ and apply the Caudy residue theorem, then (B.10) becomes

$$U(r,\theta) = \frac{M}{2} \sum_{\nu} \frac{(\nu + \frac{1}{2})}{\sin \nu\pi} \frac{P_\nu(\cos(\pi - \theta))}{\left(\frac{dW_s}{ds}\right)_{s=\nu}} \begin{cases} Q_\nu(b)\, V_\nu(r) \\ V_\nu(b)\, Q_\nu(r) \end{cases} + I_1 \qquad (B.11)$$

where ν represents the zeros of W_s in the lower half of the complex s-plane.

It can be shown that if the earth is assumed to be a perfect conductor, then the integral I_1 vanishes identically. If the earth is not a perfect conductor, I_1 will not be zero. However, it can be shown that I_1 is small compared to the first term of the series in (B.11) as long as the dielectric constant of the earth is large compared to the dielectric constant of the atmosphere. So that finally,

$$U(r,\theta) = \frac{M}{2} \sum_{\nu} \frac{\nu + \frac{1}{2}}{\sin \nu\pi} \frac{P_\nu (\cos (\pi - \theta))}{\left(\frac{dW_s}{ds}\right)_{s=\nu}} \begin{cases} Q_\nu(b)\, V_\nu(r) & r \leq b \\ Q_\nu(r)\, V_\nu(b) & r \geq b \,. \end{cases} \tag{B.12}$$

APPENDIX C

DERIVATION OF EQUATIONS (4.12) and (4.13)

From equation (4.4), consider the following two equations:

$$\frac{d^2}{dr^2}(rV_t) + \left[k^2 - \frac{t(t+1)}{r^2}\right](rV_t) = 0 \tag{C.1}$$

and

$$\frac{d^2}{dr^2}(rQ_\nu) + \left[k^2 - \frac{\nu(\nu+1)}{r^2}\right](rQ_\nu) = 0 \quad . \tag{C.2}$$

Here t is any value and is not an eigenvalue. Multiply (C.1) by (rQ_ν) and (C.2) by (rV_t), subtract and integrate with respect to r from r = a to r = ∞. We obtain

$$(\nu - t)(t+\nu+1)\int_a^\infty V_t Q_\nu dr = rV_t \frac{d}{dr}(rQ_\nu) - (rQ_\nu)\frac{d}{dr}(rV_t)\Big|_a^\infty . \tag{C.3}$$

Substitution of (4.8) for the lower limit in (c.3) results in its vanishing. Hence, considering the right side of (C.3) at its upper limit as $t \to \nu$ results in

$$\int_a^\infty V_\nu Q_\nu dr = \lim_{\substack{r\to\infty \\ t\to\nu}} \left[\frac{(rV_t)(rQ_\nu)' - (rQ_\nu)(rV_t)'}{\nu(\nu+1) - t(t+1)}\right] . \tag{C.4}$$

The numerator vanishes since it reduces to the Wronskian W_ν as $t \to \nu$. This also implies that

$$V_\nu = \alpha_\nu Q_\nu \tag{C.5}$$

as was pointed out previously. Then applying L' Hospital's rule to (C.4) results in

$$\int_a^\infty V_\nu Q_\nu \, dr = \lim_{r\to\infty} \frac{\left.\frac{dW_t}{dt}\right|_{t=\nu}}{-(2\nu + 1)} \quad . \tag{C.6}$$

Since the Wronskain of any two independent functions is a constant (C.6) reduces to

$$\int_a^\infty V_\nu Q_\nu dr = - \frac{\left.\frac{dW_t}{dt}\right|_{t=\nu}}{(2\nu + 1)} \quad .$$

Making use of (C.5), we have

$$\left.\frac{dW_t}{dt}\right|_{t=\nu} = - \frac{V_\nu(r)}{Q_\nu(r)} \quad (2\nu + 1) \int_c^\infty (Q_\nu)^2 \, dr \tag{C.7}$$

And substituting (C.7) in the expression for $U(r,\theta)$, we have

$$U(r,\theta) = \frac{-M}{4} \sum_\nu \frac{Q_\nu(b)\, Q_\nu(r)}{\int_a^\infty (Q_\nu(r))^2 \, dr} \cdot \frac{P_\nu\,(\cos\,(\pi - \theta))}{\sin \nu\pi} \quad \text{for } r \geq a. \tag{C.8}$$

The integral in the denominator is numerically inconvenient. To simplify (C.8) consider the expression (C.3) again

$$\int_a^\infty V_t Q_\nu \, dr = \frac{(rV_t) \frac{d}{dr} (rQ_\nu) - (rQ_\nu) \frac{d}{dr} (rV_t)}{\nu(\nu + 1) - t(t + 1)} \Bigg|_a^\infty \tag{C.9}$$

and using (C.5) as

$$V_t = \alpha_t Q_t \quad ,$$

then the normalized integral is

$$\int_a^\infty (Q_\nu)^2 \, dr = \lim_{t\to\nu} \frac{Q_t(r)}{V_t(r)} \left\{ \frac{(rV_t)\frac{d}{dr}(rQ_\nu) - (rQ_\nu)\frac{d}{dr}(rV_t)}{\nu(\nu+1) - t(t+1)} \right\} \Bigg|_a^\infty . \quad (C.10)$$

Differentiating numerator and denominator with respect to t, and remembering that when $t = \nu$, an eigenvalue, the function $V_t(r)$ is identical with $Q_t(r)$.

Hence,

$$\int_a^\infty (Q_\nu)^2 \, dr = \lim_{t\to\nu} \frac{\frac{\partial}{\partial t}(rV_t)\left|\frac{d}{dr}(rQ_\nu) - (rQ_\nu)\frac{d}{dr}(rV_t)\right|}{\frac{\partial}{\partial t}\left|\nu(\nu+1) - t(t+1)\right|} \Bigg|_a^\infty . \quad (C.11)$$

The denominator of (C.11) is simply $-(2t + 1)$. The numerator is

$$\lim_{t\to\nu} \left\{ (rV_t)\frac{\partial}{\partial t}\frac{d}{dr}(rQ_\nu) + \frac{d}{dr}(rQ_\nu)\frac{\partial}{\partial t}(rV_t) - (rQ_\nu)\frac{\partial}{\partial t}\frac{d}{dr}(rV_t) \right.$$

$$\left. - \frac{d}{dr}(rV_t)\frac{\partial}{\partial t}(rQ_\nu) \right\} \quad (C.12)$$

evaluated at $r = a$ and $r = \infty$. Now since the right hand side of (4.11) is independent of t, we have

$$\frac{\partial}{\partial t} \cdot \frac{\frac{d}{dr}(rV_t)}{(rV_t)} \Bigg|_{r=a} = 0 \quad (C.13)$$

or

$$(rV_t)\frac{\partial}{\partial t}\frac{d}{dr}(rV_t)\Big|_{r=a} - \frac{\partial}{\partial t}(rV_t)\frac{d}{dr}(rV_t)\Big|_{r=a} = 0 \qquad (C.14)$$

or since when $t = \nu$ the function $V_\nu(r)$ is identical with $Q_\nu(r)$, then

$$(rQ_\nu)\frac{\partial}{\partial t}\frac{d}{dr}(rV_\nu)\Big|_{r=a} - \frac{\partial}{\partial t}(rV_\nu)\frac{d}{dr}(rQ_\nu) = 0 \quad . \qquad (C.15)$$

Using this in (C.12) we obtain for the right hand side of (C.11)

$$\int_a^\infty (Q_\nu)^2\,dr = \frac{(rQ_\nu)\frac{\partial}{\partial t}\frac{d}{dr}(rQ_\nu) - \frac{d}{dr}(rQ_\nu)\frac{\partial}{\partial t}(rQ_\nu)}{-(2\nu+1)}\Bigg|_a^\infty \qquad (C.16)$$

The numerator vanishes as $t\to\infty$. If $Q_\nu(a) \neq 0$, that is, the earth is not a perfect conductor, then we can write

$$\int_a^\infty Q^2(r)\,dr = \frac{-1}{(2\nu+1)}\left[(rQ_t)^2\frac{\partial}{\partial t}\left(\frac{\frac{d}{dr}(rQ_t)}{rQ_t}\right)\right]_{\substack{r=a\\t=\nu}} \quad . \qquad (C.17)$$

If the earth is a perfect conductor then from (4.10)

$$(rV_\nu)\Big|_{r=a} = 0 \qquad (C.18)$$

and remembering that as $t\to\nu$, $V_\nu = Q_\nu$ we have from (C.12) that

$$\int_a^\infty Q^2(r)\, dr = \frac{-1}{(2\nu + 1)} \left[\frac{d}{dr} (rQ_t) \frac{d}{dt} (rQ_t) \right]_{\substack{r=a \\ t=\nu}} \tag{C.19}$$

for the perfectly conducting earth.

Using (C.17) and (C.19) in the expression for the boundary condition (4.11) and (4.10), we obtain expressions (4.12) and (4.13).

APPENDIX D

THE MODIFIED HANKEL FUNCTIONS AND THEIR PROPERTIES

The differential equation

$$\frac{d^2u}{dz^2} + z\,u = 0 \tag{D-1}$$

is known as Stokes' equation and general solutions can be written in terms of Bessel functions of order one-third [22]. The only singularity of this equation is an irregular singularity at infinity. Equation (D-1) has solutions $h_1(z)$ and $h_2(z)$ which can be written in terms of the two Bessel functions of the third kind of order one-third as follows:

$$h_1(z) = \left(\frac{2}{3} z^{3/2}\right)^{1/3} H^{(1)}_{1/3}\left(\frac{2}{3} z^{3/2}\right) \tag{D-2}$$

$$h_2(z) = \left(\frac{2}{3} z^{3/2}\right)^{1/3} H^{(2)}_{1/3}\left(\frac{2}{3} z^{3/2}\right) \tag{D-3}$$

$H^{(1)}_{1/3}(x)$ and $H^{(2)}_{1/3}(x)$ are triple valued functions of x, with a branch point at the origin. However, the product of the two multiple-valued functions $\left(\frac{2}{3} z^{3/2}\right)^{1/3}$ and $H^{(j)}_{1/3}\left(\frac{2}{3} z^{3/2}\right)$ is the single valued function $h_j(z)$. The Wronskian of h_1 and h_2, $W(h_1, h_2)$ has an identically vanishing derivative, so that

$$W(h_1, h_2) = -\frac{4i}{\pi}\left(\frac{3}{2}\right)^{1/3}$$

$$= -1.\ 457\ 495\ 441\ 040\ 461\ i \tag{D-4}$$

a constant.

The solution $h_1(z)$ and $h_2(z)$ are also related to the Airy integrals Ai(z) and Bi(z), defined for real values of z by

$$Ai(-z) = \frac{1}{\pi}\int_0^\infty \cos\left(\frac{t^3}{3} - zt\right) dt \qquad \text{(D-5)}$$

$$B_i(-z) = \frac{1}{\pi}\int_0^\infty \left[e^{-t^3/3 - zt} + \sin\left(\frac{t^3}{3} - zt\right) dt\right] \qquad \text{(D-6)}$$

Then

$$h_1(z) = k\left[Ai(-z) - i\, Bi(-z)\right] \qquad \text{(D-7)}$$

$$h_2(z) = k^*\left[Ai(-z) + i\, Bi(-z)\right] \qquad \text{(D-8)}$$

$$Ai(z) = \frac{1}{2k} h_1(-z) + \frac{1}{2k^*} h_2(-z) \qquad \text{(D-9)}$$

$$Bi(z) = \frac{i}{2k} h_1(-z) - \frac{1}{2k^*} h_2(-z) \qquad \text{(D-10)}$$

where

$$k = \left(\frac{3}{2}\right)^{2/3}\left(1 - \frac{i\sqrt{3}}{3}\right)$$

or

$$k = 1.310\ 370\ 697\ 104\ 448 - 0.756\ 542\ 874\ 711\ 451\ i$$

and

$$\frac{1}{2k} = 0.286\ 178\ 560\ 638\ 333 + 0.165\ 225\ 269\ 020\ 841\ i$$

and the star denotes complex conjugate.

Asymptotic Expansions

The asymptotic expansion of $h_1(z)$ for $-\frac{2\pi}{3} < \arg z < \frac{4\pi}{3}$,

$$h_1(z) \sim \alpha\, z^{-1/4}\, e^{2/3i\, z^{3/2} - \frac{5\pi i}{12}} \left[1 + \sum_{m=1} (-i)^m\, C_m\, z^{-3m/2}\right], \tag{D-11}$$

$$C_m = \frac{(9-4)(81-4)\ \ldots\ (9\,[2m-1]^2 - 4)}{2^{4m}\, 3^m\, m!}$$

This expression cannot be used along the ray, $\arg z = -\frac{2\pi}{3}$. This ray is the branch-cut for the multiple valued functions. The numerical coefficient is

$$\alpha = 2^{1/3}\, 3^{1/6}\, \pi^{-1/2} = 0.853\ 667\ 218\ 838\ 951.$$

An asymptotic expansion valid on the ray, $\arg z = -\frac{2\pi}{3}$ is

$$h_1(z) \sim \alpha\, z^{-1/4}\, e^{2/3i\, z^{3/2} - \frac{5\pi i}{12}} \left[1 + \sum_{m=1} (-i)^m\, C_m\, z^{-3m/2}\right] \tag{D-12}$$

$$+ \alpha\, z^{-1/4}\, e^{-2/3i\, z^{3/2} - \frac{11\pi i}{12}} \left[1 + \sum_{m=1} (i)^m\, C_m\, z^{-3m/2}\right]$$

This expansion holds for $-\frac{4\pi}{3} < \arg z < 0$; the branch cut for the fractional powers of z can be drawn anywhere within the sector $0 < \arg z < \frac{2\pi}{3}$.

The existence of two expressions of different forms which represent asymptotically the same integral function, $h_1(z)$, is an example of Stokes'

phenomenon.

The region $\frac{2\pi}{3} < \arg z < \frac{4\pi}{3}$ for (D-11) coincides with the region $-\frac{4\pi}{3} < \arg z < -\frac{2\pi}{3}$ for (D-12). Thus in this region, we use arg z = a in (D-11) and arg z = a - 2π in (D-12) with $\frac{2\pi}{3} < a < \frac{4\pi}{3}$.

The asymptotic expansions for $h_2(z)$ are

$$h_2(z) \sim \alpha\, z^{-1/4}\, e^{-2/3i\, z^{3/2} + \frac{5\pi i}{12}} \left[1 + \sum_{m=1} (i)^m\, C_m\, z^{-3m/2}\right] \tag{D-13}$$

valid for $-\frac{4\pi}{3} < \arg z < \frac{2\pi}{3}$, and

$$h_2(z) \sim \alpha\, z^{-1/4}\, e^{-2/3i\, z^{3/2} + \frac{5\pi i}{12}} \left[1 + \sum_{m=1} (i)^m\, C_m\, z^{-3m/2}\right] \tag{D-14}$$

$$+ \alpha\, z^{-1/4}\, e^{2/3i\, z^{3/2} + \frac{11\pi i}{12}} \left[1 + \sum_{m=1} (-i)^m\, C_m\, z^{-3m/2}\right]$$

valid for $0 < \arg z < \frac{4\pi}{3}$.

Special Properties of $h_1(z)$ and $h_2(z)$

The zeros of $h_1(z)$ and those of $h_1'(z)$ lie on the ray of slope $-\frac{2\pi}{3}$, while those of $h_2(z)$ and of $h_2'(z)$ lie on the ray of slope angle $\frac{2\pi}{3}$. The zeros of all these functions are simple.

If

$$T = \frac{2}{3}\, z^{3/2} \qquad \text{and} \qquad z = \left(\frac{3}{2}\, T\right)^{2/3} \tag{D-15}$$

with

$$\arg z = \frac{2}{3} \arg T \tag{D-16}$$

Then

$$H_{1/3}^{(1)}(T) = T^{-1/3} h_1(z) \tag{D-17}$$

$$H_{1/3}^{(2)}(T) = T^{-1/3} h_2(z) \tag{D-18}$$

and

$$H_{2/3}^{(1)}(T) = \left(\frac{2}{3}\right)^{1/3} e^{-\frac{2\pi i}{3}} T^{-2/3} h_1'(z) \tag{D-19}$$

$$H_{2/3}^{(2)}(T) = \left(\frac{2}{3}\right)^{1/3} e^{+\frac{2\pi i}{3}} T^{-2/3} h_2'(z) \tag{D-20}$$

Figures D-1 and D-2 give the regions of validity of the asymptotic expansions of $h_1(z)$ and $h_2(z)$.

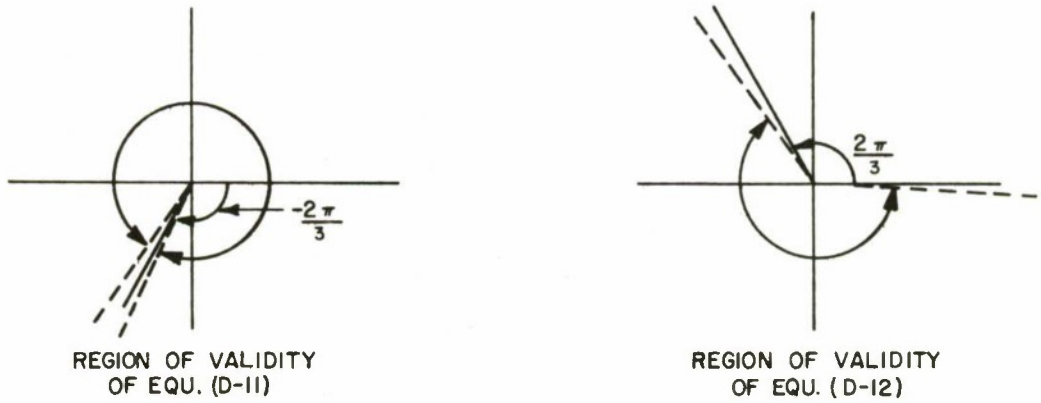

REGION OF VALIDITY OF EQU. (D-11)

REGION OF VALIDITY OF EQU. (D-12)

Figure D-1 . REGIONS OF VALIDITY OF THE ASYMPTOTIC EXPANSION FOR $h_2(z)$

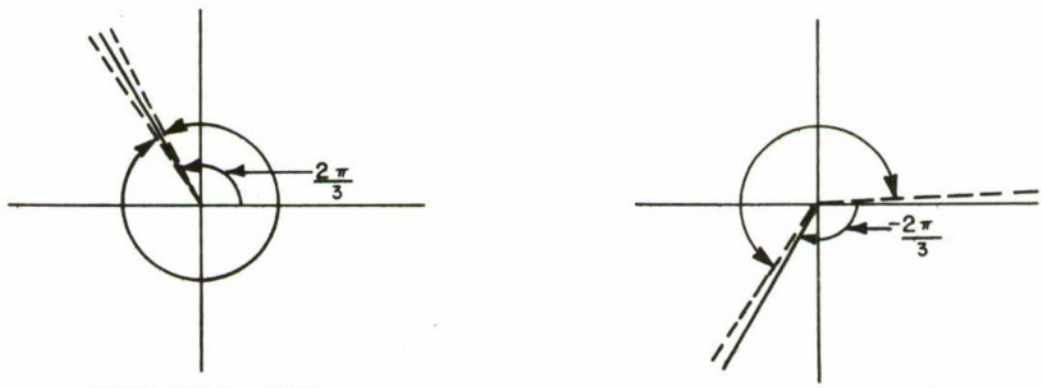

REGION OF VALIDITY OF EQU. (D-13)

REGION OF VALIDITY OF EQU. (D-14)

IA-37,815

Figure D-2. REGIONS OF VALIDITY OF THE ASYMPTOTIC EXPANSIONS OF $h_2(z)$

BIBLIOGRAPHY

1. Bratt, P., Covitt, A., Dresp, M., et al, "CNI Experimental Test Program Plan," The MITRE Corp. Technical Report, MTR-2282, ESD-TR-72-136, 7 January 1972

2. Wong, M. S., "Refraction Anomalies in Airborne Propagation," Proc. IRE 46, September 1958, pp. 1628-1638

3. Furry, W. H., "Theory of Characteristics Functions in Problems of Anomalous Propagation," O.E.M., Sr-262, Division 14, Rept. 680, MIT Radiation Lab., 28 February 1945

4. Northover, F. H., Applied Diffraction Theory, American Elsevier Publ. Co., N.Y. 1971

5. Chang, H. T., "The Effect of Tropospheric Layer Structures on Long-Range VHF Radio Propagation," IEEE Trans. Ant. and Prop. AP-19, No. 6, pp. 751-756, November 1971

6. Langer, R. E., "On the Connection Formulas and the Solutions of the Wave Equation," Physical Review, 51, p. 669, April 1937

7. Pekeris, C. L., "The Accuracy of the Earth Flattering Approximation in the Theory of Microwave Propagation," Physical Review 70, No. 7 and 8, October 1 and 15, 1946, p. 518

8. Livingston, D. C., The Physics of Microwave Propagation, Prentice Hall, N. J., 1970

9. "Investigation of Air-to-Air and Air-to-Ground Electromagnetic Propagation," School of EE, Cornell University, Research Dept. EE 138, Parts III, IV and V, 1951-1952.

10. "UHF Propagation Tests Over Land and Water," U.S. Naval Air Test Center, Patuxent River, Maryland, PTR EL-929, 1 December 1949

Bibliography (Concluded)

11. "An Investigation of Airborne Microwave--Marcom Relay Final Report," Vol. I and II, Tech. Rept. SEG-TR-66-31, by Collins Radio Co., Systems Engineering Div. Dallas Texas, 1966

12. Friedman, B., "Propagation in a Non-Homogeneous Atmosphere," in The Theory of Electromagnetic Waves, Ed M. Kline, Dover Publ., Inc. N. Y. 1951

13. Watson, G. N., "The Diffraction of Electric Waves by the Earth," Proc. Roy, Soc. London, A95 (1918), pp. 83-99
Watson, G. N., "The Transmission of Electric Waves Around the Earth," Proc. Roy. Soc. London, A95 (1919), pp. 546-562

14. Doviak, R. and Goldhirsh, J., "Radiation Due to a Magnetic Dipole in a Spherically Inhomogeneous Medium," Independent Research Program, Raytheon Co., BR-2792, 31 December 1963

15. Bremmer, H., Terrestial Radio Waves, Elsevier Publ. Co., N. Y., Houston 1949

16. Furry, W. H., "Methods of Calculating Characteristic Values for Bilinear M Curves," Rept. 795, MIT Radiation Lab., 6 February 1945

17. Beckett, R. and Hurt, J., Numerical Calculations and Algorithms, McGraw Hill Co., N. Y. 1967

18. Northover, F. H., "Long Distance VHF Fields," Parts I, II and III, Canadian Journal of Physics 33, May/June 1955, p. 241

19. Kerr, D. E., Propagation of Short Radio Waves, MIT Radiation Lab. Series, Vol. 13, 1951

20. Katzin, M., et al, "The Trade Wind Inversion as a Transoceanic Duct," J. Research N. B. S. Vol. 64D, No. 3, May-June 1960, p. 247

21. Ament, W. S., Katzin, M., and Ringwalt, D. L., "The Communications Potentialities of the Trade Wind Inversion Duct-Analysis of Project NEPTUNE Data," Rept. CRL-272-2, 31 July 1963

22. Modified Hankel Function of Order One Third, Vol. II, Harvard Computation Laboratory, Harvard Univ. Press, Cambridge, Mass., 1945

Security Classification

DOCUMENT CONTROL DATA - R & D

(Security classification of title, body of abstract and indexing annotation must be entered when the overall report is classified)

1. ORIGINATING ACTIVITY (Corporate author)	2a. REPORT SECURITY CLASSIFICATION
The MITRE Corporation P.O. Box 208 Bedford, Mass. 01730	UNCLASSIFIED 2b. GROUP

3. REPORT TITLE

RADIO WAVE PROPAGATION IN THE PRESENCE OF A TROPOSPHERIC DUCT

4. DESCRIPTIVE NOTES (Type of report and inclusive dates)

5. AUTHOR(S) (First name, middle initial, last name)

M. R. Dresp

6. REPORT DATE	7a. TOTAL NO. OF PAGES	7b. NO. OF REFS
DECEMBER 1972	104	22

8a. CONTRACT OR GRANT NO.	9a. ORIGINATOR'S REPORT NUMBER(S)
F19628-71-C-0002	
b. PROJECT NO. 511A	ESD-TR-72-323
c.	9b. OTHER REPORT NO(S) (Any other numbers that may be assigned this report) MTR-2455
d.	

10. DISTRIBUTION STATEMENT

Approved for public release; distribution unlimited.

11. SUPPLEMENTARY NOTES	12. SPONSORING MILITARY ACTIVITY
	Deputy for Planning and Technology Electronic Systems Division (AFSC) L. G. Hanscom Field, Bedford, Mass. 01730

13. ABSTRACT

A full-wave solution has been obtained for radio wave propagation in the presence of an elevated tropospheric layer. This analysis was performed as part of the CNI (Communication, Navigation, Identification) experimental program. The tropospheric layer is modeled as a trilinear refractive index profile with a sufficient lapse rate so as to result in an elevated duct. The analytical solutions give the received signal level for air-to-air propagation paths at UHF, the corresponding signal fading level, and the space diversity distance to insure good quality reception. The analysis performed here can be applied to ionospheric propagation and to the underwater acoustic channel.

DD FORM 1 NOV 65 1473

Security Classification

14. KEY WORDS	LINK A		LINK B		LINK C	
	ROLE	WT	ROLE	WT	ROLE	WT
IONOSPHERIC PROPAGATION						
TROPOSPHERE MODELING						
TROPOSPHERIC PROPAGATION						
WAVE PROPAGATION						